25/1173

NUREG/CR-1173

An Experimental Study of Turbulent Thermal Convection with Time-Dependent Volumetric Energy Sources

JAN 8 1980
U. S. GOVT. PUBS.
DEPOSITORY

Prepared by M. Keyhani, F. A. Kulacki

The Ohio State University Research Foundation

Prepared for
U. S. Nuclear Regulatory
Commission

Y 3.N 88:

NOTICE

This report was prepared as an account of work sponsored by an agency of the United States Government. Neither the United States Government nor any agency thereof, or any of their employees, makes any warranty, expressed or implied, or assumes any legal liability or responsibility for any third party's use, or the results of such use, of any information, apparatus product or process disclosed in this report, or represents that its use by such third party would not infringe privately owned rights.

Available from

GPO Sales Program
Division of Technical Information and Document Control
U. S. Nuclear Regulatory Commission
Washington, D. C. 20555

and

National Technical Information Service
Springfield, Virginia 22161

NUREG/CR-1173
R3

An Experimental Study of Turbulent Thermal Convection with Time-Dependent Volumetric Energy Sources

Manuscript Completed: September 1979
Date Published: December 1979

Prepared by
M. Keyhani, F. A. Kulacki

The Ohio State University Research Foundation
Department of Mechanical Engineering
Columbus, OH 43201

Prepared for
Division of Reactor Safety Research
Office of Nuclear Regulatory Research
U.S. Nuclear Regulatory Commission
Washington, D.C. 20555
NRC FIN No. A4061

ABSTRACT

Transient natural convection in a horizontal layer of dilute aqueous electrolyte with uniform internal heat generation is experimentally investigated. The objectives of the investigation are to sharpen the results reported by Kulacki and Emara [9] in an earlier investigation and to determine the time to reach steady state when the internal heat generation rate undergoes a step change which takes the layer from one state of steady convection to another. Both developing and decaying flows are investigated by measurement of the temporal history of the maximum temperature difference across the layer as the volumetric heat generation rate is varied in this manner. The layer is bounded from below by a rigid, zero heat flux surface and from above by a rigid, isothermal surface.

For developing flows, with an initial Rayleigh number of zero, the present results confirm the earlier experimental data of Kulacki and Emara. Also, when the initial state of motion is not zero and the Rayleigh number is increased, the flow development time is in good agreement with the data of Kulacki and Emara and the recent analytical work of Cheung [5]. However, first-order time constants obtained in the present study are slightly larger than those obtained by Kulacki and Emara. This difference can be explained, in part, by the difference in the techniques used to record the maximum temperature difference in the two studies.

In decaying flows, the cases of a zero and non-zero final Rayleigh number exhibit longer flow transients than the results reported by Kulacki and Emara. The present results are, moreover, in good agreement with Cheung's prediction, which is based on a boundary layer analysis of the transient process. A correlation between the Fourier number and the normalized step decrease in the Rayleigh number is given by

$$Fo_{max,cooling} = 1.046 \left(\frac{\Delta Ra}{\theta_{co_F}} \right)^{-0.0778},$$

where

$$10^8 \leq \frac{\Delta Ra}{\theta_{co_F}} \leq 10^{11},$$

Fo is defined as $\alpha t/L^2$, Ra is the Rayleigh number based on the conduction temperature modulus with uniform internal energy generation, and θ_{co_F} is the final, steady-state maximum temperature difference in the layer.

The present correlation for flow decay time is in fair agreement with the results of Kulacki and Emara for large time. For small time, experimental uncertainties indicate a possible correction of 15% to 20% in temperature. This will bring the present results only slightly closer to the early flow development trends in temperature observed by Kulacki and Emara, where present data indicate a larger first order time constant. Thus, the present correlation for flow decay time may be considered an improvement of the earlier result reported by Kulacki and Emara.

TABLE OF CONTENTS

		Page
ABSTRACT		i
LIST OF FIGURES		iv
LIST OF TABLES		vi
NOMENCLATURE		vii
Section		
I	INTRODUCTION	1
	A. Overview	1
	B. Literature Review	2
	C. Objectives of the Present Study	11
II	EXPERIMENTAL APPARATUS AND PROCEDURE	12
	A. Experimental Apparatus	12
	B. Experimental Procedure	16
III	PRESENTATION AND DISCUSSION OF RESULTS	18
	A. Steady State Heat Transfer	18
	B. Convection Transient	18
IV	CONCLUSION	44
APPENDIX A -	THERMOPHYSICAL PROPERTIES	47
APPENDIX B -	EXPERIMENTAL DATA	49
APPENDIX C -	ANALYSIS OF EXPERIMENTAL EFFORTS	56
BIBLIOGRAPHY		58

LIST OF FIGURES

Figure		Page
1	Schematic of Fluid Layer and the Thermal Boundary Layer	7
2	Time Dependence of the Exponent of the Boundary Layer Relation	10
3	Detail View of Convection Cell	13
4	Schematic Diagram of Apparatus and Instrumentation	15
5	Steady-State Nusselt Numbers Obtained from Asymptotic Values of the Temperature Difference Following a Step Change in Rayleigh Number	19
6	Steady-State, Non-Dimensional Temperature Difference Data	20
7	Typical Thermocouple Response Versus Time and Definition of t_σ and t_{max}	22
8	Step Change in the Rayleigh Number Versus the Fourier Number with the Initial Dimensionless Core Temperature as the Parameter in the Developing Flow	23
9	Step Change in the Rayleigh Number Versus the Fourier Number with the Initial Dimensionless Core Temperature as the Parameter in the Decaying Flow	24
10	Fourier Numbers for Developing Flow Compared to the Predictions of Cheung [5].	25
11	Fourier Numbers for Decaying Flow Compared to the Predictions of Cheung [5].	26
12	Family of Curves Representing Step Increase in the Rayleigh Number Versus the Fourier Number	28
13	Family of Curves Representing Step Decrease in the Rayleigh Number Versus the Fourier Number	29
14	Step Increase in the Rayleigh Number Versus Dimensionless Time	30
15	Step Decrease in the Rayleigh Number Versus Dimensionless Time	31

READEX FICHE best copy available

LIST OF FIGURES - (Continued)

Figure		Page
16	Normalized Step Increase in the Rayleigh Number Versus Dimensionless Time. Predictions of Cheung [5] Give the Range of Fourier Number Where the Maximum Temperature Difference is Within Two Percent of the Final Steady-State Value ($Fo_{98\%} \leq Fo \leq Fo_{max}$)	33
17	Normalized Step Decrease in the Rayleigh Number Versus Dimensionless Time. Predictions of Cheung [5] Give the Range of Fourier Number Where the Minimum Temperature Difference is Within Two Percent of the Final Steady-State Value ($Fo_{98\%} \leq Fo \leq Fo_{max}$)	34
18	Correlations for Step Decrease in the Rayleigh Number Versus the Fourier Number	37
19	Normalized Step Increase in the Rayleigh Number Versus the Fourier Number of the Pseudo First-Order Time Constant for the Minimum Temperature Difference Within the Layer	38
20	Normalized Step Decrease in the Rayleigh Number Versus the Fourier Number of the Pseudo First-Order Time Constant for the Minimum Temperature Difference Within the Layer	39
21	Measured and Predicted Temperature Difference Across the Layer for a Step Increase in Rayleigh Number. The Prediction is Based on the Boundary Layer Analysis of Cheung [5].	40
22	Measured and Predicted Temperature Difference Across the Layer for a Step Decrease in Rayleigh Number. The Prediction is Based on the Boundary Layer Analysis of Cheung [5].	41
23	Maximum Temperature Difference for the Complete Decay of Turbulent Convection	42

LIST OF TABLES

Table		Page
A-1	Thermophysical Property Values of Water	48
B-1	Steady State Heat Transfer Data	50
B-2	Data for Developing Flow for a Step Increase in Rayleigh Number, $Ra_I = 0$	52
B-3	Data for Decaying Flow for a Step Decrease in Rayleigh Number, $Ra_F = 0$	53
B-4	Data for Developing Glow for a Step Increase in Rayleigh Number, $Ra_I > 0$	54
B-5	Data for Decaying Flow for a Step Decrease in Rayleigh Number $Ra_F > 0$	55

NOMENCLATURE

A	Area of heat transfer surface
c_p	Specific heat
f	Fractional error
F_o	Fourier number
g	Constant of gravitational acceleration
H	Volumetric energy source strength
h	Convective heat transfer coefficient
k	Thermal conductivity
l	Thickness of lower plate
L	Thickness of fluid layer
m	Exponent of the boundary layer relation, defined by Eq. (19)
n	Exponent of correlation for heat transfer measurements
Nu	Nusselt number, $\frac{(P - P_L)L}{kA\Delta T} \equiv \frac{hL}{k}$
P	Power input to the fluid layer
P_L	Power output from fluid layer
Pr	Prandtl number, $\frac{\nu}{\alpha}$
Q	Heat flux at the upper surface
Ra	Rayleigh number, $(\frac{g\beta}{\alpha\nu})L^3(\frac{HL^2}{2k})$
ΔRa	Step change in the Rayleigh number
t	Time
T	Mean temperature
T'	Fluctuating temperature
ΔT	Temperature difference across fluid layer

v Vertical component of velocity

W Weight percent of copper sulfate

Z Vertical distance from lower surface, $0 \leq Z \leq L$

Greek Symbols

α Thermal diffusivity, $\alpha = \frac{k}{\rho c_p}$

δ Thermal boundary layer thickness

ρ Density

θ Dimensionless temperature, $\frac{2k(T - T_1)}{HL^2}$

ν Kinematic viscosity

β Coefficient of thermal expansion

Subscripts

c Value at critical point

co Value at turbulent core

F Final condition

I Initial condition

o Value at lower surface of fluid layer

1 Value at the upper surface of fluid layer

Superscripts

$'$ Fluctuating quantity

$\overline{}$ Horizontal average

I. INTRODUCTION

A. OVERVIEW

Turbulent natural convection in an internally heated fluid layer has recently received emphasis because of its connection with certain aspects of post-accident heat removal following a core melt accident in nuclear power reactors. In the final phase of such an accident, a layer or molten pool of energy generating fluid is formed at the bottom of the reactor containment vessel or in an ex-vessel barrier/containment. The fission products present in the melt generate heat at a high power level, and, consequently, heat-source driven natural convection at high Rayleigh numbers can be expected in the layer. In most cases, the volumetric heat generation rate, which controls the convective motion of the layer, is a function of time owing to fission product decay. This time dependence of the flow and temperature has a significant effect on heat transfer within the melt. Knowledge of the transient thermal behavior of the melt layer is needed in order to estimate the thermal loading on the barrier structure or a molten core retention device.

The transient thermal behavior and boundary heat fluxes of the melt layer can be investigated via two possible transport mechanisms; the first is based on thermal convection, and the second on internal radiation. In the first case, turbulent thermal convection is the dominant mechanism. The radiation-dominated model has been suggested by a study of heat transfer in molten pools of UO_2 [1]* and is based on optically thick internal radiation averaged overall wavelengths, neglecting the simultaneous occurence of thermal convection. This model, in effect, leads to the study of heat conduction in a rectangular parallelopiped with a temperature-dependent thermal conductivity and internal heat generation.

Thermal convection driven by internal energy generation can play an important role in heat transport processes encountered in astrophysics and geophysics. Natural convection problems can also be encountered in geophysical processes, such as buoyancy induced motion in the earth's mantle [17,23] as a result of radioactive heat generation within the continental crust. Convection with internal heating may also be the origin of the cellular arrays in the atmosphere of Venus observed by Mariner 10 [21].

In the present study, a convection model with a low temperature fluid is chosen for the investigation of the transient thermal behavior of an internally heated layer. The model fluid is dilute aqueous

---

* Numbers in brackets denote references listed in the Bibliography.

electrolyte with uniform volumetric energy generation provided by Joule heating. The layer is bounded from below by a rigid, adiabatic surface and from above by a rigid, isothermal surface.

B. LITERATURE REVIEW

Research performed in the area of natural convection in internally heated fluid layers has been both experimental and theoretical. Experimental studies have been both qualitative and quantitative in nature. The qualitative experiments were primarily concerned with the nature of the flow field, while steady-state heat transfer measurements at the boundaries was the objective of the quantitative studies. Most previous theoretical investigations in a horizontal fluid layer with internal energy generation attempted to determine average heat fluxes at the layer boundaries in terms of the Rayleigh number, to obtain the critical Rayleigh number for the onset of convection, or to gather information about the temperature distribution in the layer and the form and structure of the convective motion. Very few studies of transient natural convection in a volumetrically heated fluid have been performed. The works of Kulacki and Nagle [14] and Kulacki and Emara [9] and the qualitative studies by Schwiderski and Schwab [19] and Tritton and Zarraga [22] appear to be the only existing experimental investigation of heat transport problems of this nature. The theoretical work on this problem by Cheung [5] appears to be the only existing analysis. These studies will be discussed shortly.

Since the results of the literature reviewed here are expressed in terms of Rayleigh number, it is appropriate to define the Rayleigh number at this point. For fluids satisfying the Boussinesq relation between density and temperature difference [2] the ratio of buoyant forces to viscous forces times the ratio of the heat convected to heat conducted is the characteristic dimensionless parameter and may be expressed as

$$Ra = \left(\frac{g\beta}{\alpha\nu}\right) L^3 \, \Delta T. \tag{1}$$

The quantity ΔT is characteristic destabilizing temperature difference, and L is the characteristic length scale, usually corresponding to the height of the thermally unstable portion of the layer. This dimensionless group is called the Rayleigh number in honor of Lord Rayleigh, who first used it in his analysis of hydrodynamic instability in a horizontal layer with uniform volumetric energy generation and the thermal boundary conditions of interest in the present study, the Rayleigh number can be expressed as

$$Ra = \left(\frac{g\beta}{\alpha\nu}\right) L^3 \, \left(\frac{HL^2}{2k}\right), \tag{2}$$

where $\left(\frac{HL^2}{2k}\right)$ is the maximum temperature difference for purely conductive heat transfer, and L is the thickness of the fluid layer.

Experimental Studies

Tritton and Zarraga [22] performed a qualitative study of the planform of flow in a horizontal fluid layer with volumetric energy generation. The layer was bounded from below by an insulated rigid plate, and from above by a rigid, isothermal surface. They were primarily concerned with information about the cellular convection patterns for Rayleigh numbers in the vicinity of the critical value for the onset of motion. In order to visualize the flow patterns, they used Polystyrene beads with a typical diameter of 0.03 cm. The beads fell out of the hot rising currents and rose out of the cold falling currents. It was found that the developed cellular patterns were, in many respects, similar to those of Benard convection, but with the fluid descending in cell centers and ascending at cell peripheries. The horizontal scale of the cell patterns was, in general, larger than that of Bernard convection.

An investigation similar to that of Tritton and Zarraga was performed by Schwiderski and Schwab [19]. The objective of their study was to determine the possible effect of several flow and geometrical parameters on the convection patterns. The effect of the thermal conductivity of the bottom plate was studied by interchanging the glass bottom plate with Plexiglas. It was concluded that the top and bottom boundary materials influenced the flow development time.

Krishnamurti [7] investigated the effect of a non-linear temperature field in the conduction state on the convection planforms near the critical Rayleigh number. The layer in her study did not have any internal heating source, but the change in the mean temperature was achieved by changing the boundary temperature with time. The apparatus used in this experiment allowed observations of flow patterns at Rayleigh numbers near the critical value. In the case of internal heating, where the time rate of change of temperature was positive, a hexagonal pattern with downflow in the center, was observed. On the other hand, a hexagonal pattern with up-flow in the center was observed for a negative time rate of change of mean temperature. In case of time rate of change of mean temperature across the layer being zero, and existence of a negative temperature gradient across the layer, two-dimensional rolls realized near the critical point. Subcritical instability was observed when the mean temperature was allowed to vary with a subcritical temperature difference across the layer.

Kulacki and Goldstein [12] studied the natural convection in an internally heated fluid layer bounded by two rigid horizontal plates of constant and equal temperature. Average temperature distribution within the layer was measured by interferometric methods. They found that about two-thirds of the energy transport was through upper surface; this was observed at the highest obtainable Rayleigh number with their apparatus ($Ra = 675\ Ra_c$). The heat transfer correlations for steady

convection covered the laminar, transition and turbulent regimes of flow; these correlations were,

$$Nu_1 = 0.388\ Ra^{0.236} \tag{3}$$

at the upper surface, and

$$Nu_0 = 1.524\ Ra^{0.094} \tag{4}$$

at the lower surface for $1 < Ra/Ra_c \leq 675$, where $Ra_c = 1.866 \times 10^4$. Also the extrapolation of their data yielded a critical Rayleigh number which was within +10.7% of linear stability theory predictions [11]. From the information obtained from the interferograms about the overall features of the convective flow, they concluded the following: Overall buoyant forces in the warm central core displaced this region upwards above the geometric center of the layer, for $Ra > 2642$. A quasi-periodic motion dominated the region $Ra < 1.72 \times 10^5$. Turbulent mixing effects begin to play the dominant role and any periodicity began to disappear for $Ra > 1.3 \times 10^6$.

Kulacki and Nagle [14] have reported results of a study of natural convection in a horizontal fluid layer with volumetric energy source with boundary conditions, the same as considered in the present study. The volumetric energy source was provided by Joule heating. A correlation of the average Nusselt number at the upper surface with the Rayleigh number was obtained in the form

$$Nu_1 = 0.305\ Ra^{0.239}, \tag{5}$$

for $114 \leq Ra/Ra_c \leq 1.86 \times 10^6$ ($Ra_c = 1386$ [10]) and $6.2 \leq Pr \leq 6.6$. Five discrete transitions in the heat flux were found by plotting Rayleigh number times Nusselt number versus the Rayleigh number on linear coordinates. Kulacki and Nagle also made a preliminary study of the nature of the temperature field in unsteady convection when the power is applied to an initially motionless and isothermal layer. For $Ra = 9.3 \times 10^7$, they found that for a short time after internal heating had started, a temperature overshoot, or excess, developed near the upper surface while a well-mixed isothermal core developed immediately; the temperature overshoot was believed to be caused by a dominance of conduction over convection in the vicinity of the upper surface.

Kulacki and Emara [9] also investigated heat transfer in a system similar to that of Kulacki and Nagle. A correlation of the average Nusselt number at the upper surface with the Rayleigh number was given by

$$Nu_1 = 0.396\ Ra^{0.227}, \tag{6}$$

where $1.89 \times 10^3 \leq Ra \leq 2.17 \times 10^{12}$, $2.75 \leq Pr \leq 6.86$, and $0.025 \leq L/x \leq 0.5$. This result is in close agreement with that of Kulacki and Nagle. Eight discrete transitions in the heat flux were found by plotting Rayleigh number times Nusselt number versus the Rayleigh number and linear coordinates.

Kulacki and Emara studied the development of temperature profile in the layer for the case of an on-off step function in power input. A simple relationship was given between the time required to reach the steady state and the step change in Rayleigh number for both developing and decaying convection. When a step increase in power is applied to the layer, the Fourier number required for the maximum temperature difference to reach its steady state value is given by

$$Fo_{max,heating} = 11.577 \ |\Delta Ra|^{-0.213} \tag{7}$$

When a step decrease in power is applied to the layer after steady convection has been established at a given Ra, the Fourier number required to reach an isothermal steady state is given by

$$Fo_{max,cooling} = 11.956 \ |\Delta Ra|^{-0.215} \tag{8}$$

Kulacki and Emara concluded that the time required for the layer to attain the maximum steady-state temperature difference in developing convection with internal energy sources and the time required for the decay of this temperature difference without internal energy sources are approximately the same. Thus, it appears that the governing physical parameter of the large-time behavior of either process is the maximum steady-state temperature difference within the layer. But they indicated that the initial growth and decay rates of the maximum temperature difference are quite different.

Theoretical Studies

The only existing theoretical investigation of transient thermal convection in a fluid layer with uniform volumetric energy sources appears to be the recent work of Cheung [5]. Since the results of the present study are directly comparable to Cheung's work, it is helpful to present a summary of Cheung's analysis at this point.

Cheung's theoretical analysis is based on the following considerations. Initially, the layer is in steady-state convection. Once a step change in the volumetric heat generation is applied to the layer, transition to a new steady-state occurs. Rayleigh numbers in the initial and final steady states are considered to be sufficiently high so that turbulence dominates the heat transfer during the entire transient. Except for density variation in the buoyancy force, the properties of the fluid are assumed to be constant during the transition period.

Energy production per unit volume is assumed to be the same over the entire fluid layer and the mean heat transport is assumed to be strictly one dimensional. Cheung employs two phenomenological models for analysis of transient thermal behavior of such fluid layers, the boundary layer approximation and the eddy heat transport model. The results obtained from both models, are in good agreement.

In the boundary layer approximation, the characteristic differential equation resulting from combining the continuity and energy equations and horizontally averaging is,

$$\frac{\partial T}{\partial t} + \frac{\partial}{\partial z}\left(\overline{vT'}\right) = \alpha \frac{\partial^2 T}{\partial z^2} + \frac{H}{\rho c_p}, \tag{9}$$

where $\bar{v} = 0$. The boundary conditions are,

$$\left.\frac{\partial T}{\partial z}\right|_{z=0} = 0, \text{ and } T(L) = T_1. \tag{10}$$

Experimental data indicate that for high Rayleigh numbers thermal convection between two rigid surfaces, the temperature is approximately constant over the body of the layer. In the present approach with the lower surface being thermally insulated, the overall resistance of the layer to heat transfer must therefore lie within the layer at the upper surface where a large temperature gradient exists (Fig. 1). Therefore, an approximate expression for heat flux at the upper surface can be written as follows:

$$Q = k \frac{(T_{co} - T_1)}{\delta} \tag{11}$$

Equation (10) neglects the heat generation in the thin boundary layer, δ, which results in an error of order $\frac{\delta}{L}$.

In Eq. (11), in order to determine Q, both T_{co} and δ have to be known as functions of time. At high Rayleigh numbers, the body of the fluid is at a uniform temperature of T_c. This consideration results in an error of order δ/L because of neglecting the temperature variation in the boundary layer. Integrating Eq. (9) with respect to z over the entire fluid layer, using the boundary condition at $z = 0$, and taking the above considerations into account, one obtains,

$$\rho c_p L \frac{dT_{co}}{dt} = - \frac{k(T_{co} - T_1)}{\delta} + HL, \tag{12}$$

where $\overline{vT'}$ has been eliminated by the non-slip condition at the walls. Prior to a step change in the power input to the fluid layer, the fluid

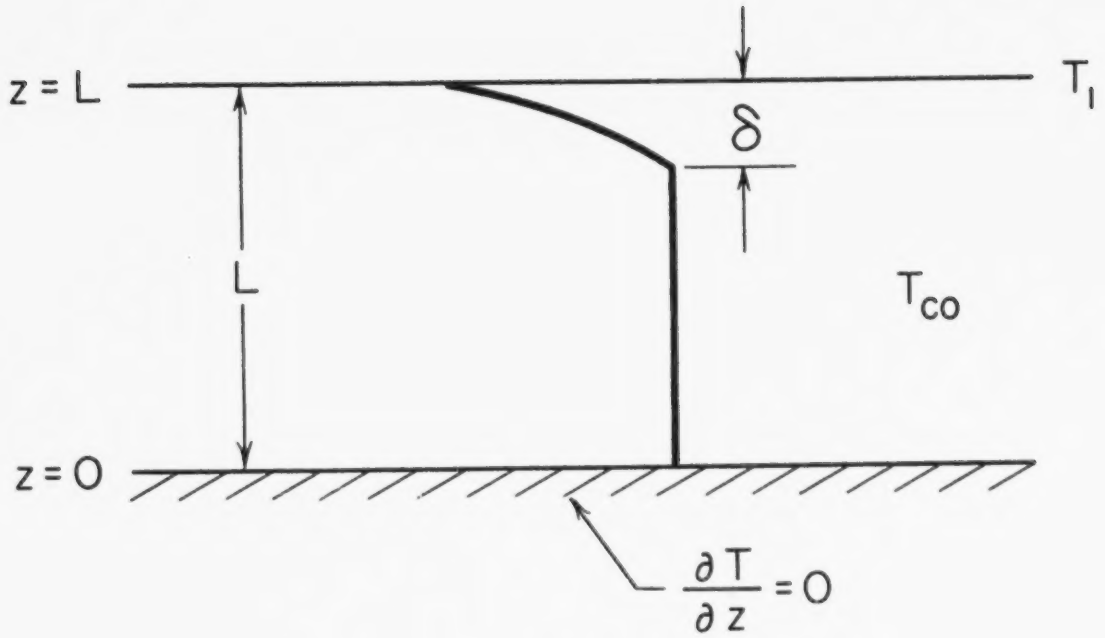

Figure 1. Schematic of Fluid Layer and the Thermal Boundary Layer

is in steady-state turbulent convection. Therefore, initially the upper surface heat flux should be the same as the total heat generation of the layer. From Eq. (11) one has,

$$H_I L = k(T_{co_I} - T_1)/\delta_I . \tag{13}$$

By dividing the Eq. (12) by Eq. (13) and simplifying one has,

$$\frac{1}{2}\frac{d\theta_{co}}{dFo} = -\frac{\theta_{co}}{\theta_{co_I}}\left(\frac{\delta}{\delta_I}\right)^{-1} + \frac{Ra_F}{Ra_I} , \tag{14}$$

where Fo is the Fourier number, $\frac{\alpha t}{L^2}$, and θ_{co} is the turbulent core temperature, $2k(T_{co} - T_1)/H_I L^2$. The volumetric internal heat generation rate, H, has been replaced by the Rayleigh number owing to the assumption of constant thermophysical properties of the fluid.

Based on existing steady-state turbulent heat transfer data [14,9], Cheung indicates that the following relationship between δ and θ_{co} exists [3]*.

$$\frac{\delta}{\delta_I} \simeq \left(\frac{\theta_{co}}{\theta_{co_I}}\right)^{-0.295} . \tag{15}$$

Cheung's argument is that, if during the flow transition the thermal boundary layer is in a quasi-steady state, the relation given by Eq.(15) should also hold instantaneously. Combining Eqs. (14) and (15), one has

$$\frac{1}{2}\frac{d\theta_{co}}{dFo} = -\left(\frac{\theta_{co}}{\theta_{co_I}}\right)^{1.295} + \frac{Ra_F}{Ra_I} . \tag{16}$$

As the experimental data of the present study became available, it was possible to verify the validity of the Eq. (15) for transient flow. In order to achieve this goal, Cheung [4] proposes the following power-law relation between δ and θ_c

$$\frac{\delta}{\delta_I} = \left(\frac{\theta_{co}}{\theta_{co_I}}\right)^{m} , \tag{17}$$

---

* In a recent study [4], Cheung introduces a modified relationship between δ and θ_c, where the exponent is changed to 0.293. This change of exponent does not produce a numerically resolvable difference in the results.

where m is assumed to be a function of time. The constant of proportionality in Eq. (17) equals unity, because at Fo = 0,

$$\frac{\delta}{\delta_I} = \frac{\theta_{co}}{\theta_{co_I}} = 1 \ . \tag{18}$$

Manipulation Eqs. (14) and (17) gives:

$$m(Fo) = \frac{\ln\left(\frac{Ra_F}{Ra_I} - 0.5\ \frac{d\theta_{co}}{dFo}\right)}{\ln\left(\frac{\theta_{co}}{\theta_{co_I}}\right)} - 1 \ , \tag{19}$$

which can be determined by experimental measurements. Cheung exployed Eq. (19) in conjunction with present experimental data [13] corresponding to the case of a step increase in Rayleigh number from 5.87×10^8 to 2.85×10^9 to derive the time dependence of m. He finds that m is a strong function of time, especially in the earlier stages of flow development. The value of m is found to be much larger than its steady-state value in the initial period of transition, but it decreases sharply at first and then gradually reaches a minimum just below the steady-state value. Thereafter, it rises slowly and eventually approaches an equilibrium value that is slightly above the steady-state value (Fig. 2).

However, the numerical solution of Eq. (16) and the experimental data are in quite satisfactory agreement, even though the steady-state value of m is used. This can be explained from a mathematical point of view. Equations (14) and (17) indicate that the rate of transition is a function of $(\theta_{co}/\theta_{co_I})^{1+m}$. Furthermore, $d\theta_{co}/dFo$ is controlled by the value of $\theta_{co}/\theta_{co_I}$ raised to a power of (1 + m), not directly to m. Therefore, in a given time step, if m is underestimated, as is the case with Eq. (16), then $d\theta_{co}/dFo$ would be slightly overestimated. Consequently, a somewhat larger value of $\theta_{co}/\theta_{co_I}$ is obtained in the next time step, where this would effect the new value of $d\theta_{co}/dFo$. Thus with $\theta_{co}/\theta_{co_I}$ being overestimated while m being underestimated, $\theta_{co}/\theta_{co_I}$ would tend to approach its true value, which in turn results in minimizing the overall error. Use of Eq. (16), in light of the compensating property of the two error sources, seems to be quite adequate for practical purposes.

The numerical solution of Eq. (16) results in the following conclusions:

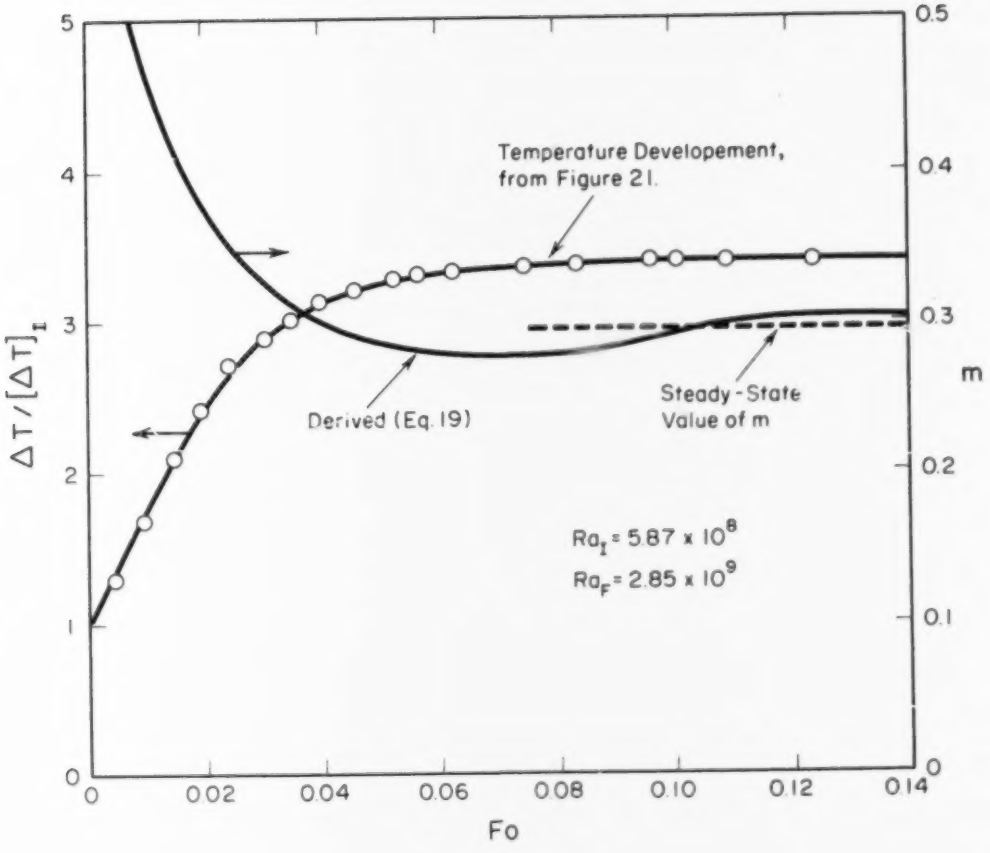

Figure 2. Time Dependance of the Exponent of the Boundary Layer Relation

1. A longer time is required for transitions with the same step change in Rayleigh number [i.e. (Ra_2-Ra_1) and $-(Ra_2-Ra_1)$] in case of decaying flow than of that of developing flow.

2. The thickness of the thermal boundary layer at the upper surface is found to be decreasing for developing flow and increasing for decaying flow.

3. In general, the time scale associated with transition from one state of steady turbulent convection to another following a step change in internal heat generation is dependent on the corresponding change in the Nusselt number at the upper surface and the initial Rayleigh number.

C. OBJECTIVES OF THE PRESENT STUDY

Previous experimental studies of thermal convection driven by internal energy sources in horizontal fluid layers with boundary conditions of interest to the present study were conducted mostly for steady-state cases. The transient experimental studies were limited to a step-change in power input, i.e. Rayleigh number, on the basis of power on-off step function. Therefore, there is a lack of experimental data for the case of transition from one state of steady convection to another following a step change in internal heat generation. One objective of the present study, thus, is to determine the time scale associated with the transition from one state of steady convection to another following a step change in internal heat generation.

Another objective of the present study is to verify the validity of the existing data [9], and to determine the differences, if any, between the developing and decaying processes. Furthermore, it is desired to verify the validity of the only existing theoretical analysis [5] which is restricted to the case of transition from one state of steady turbulent convection to another following a step change in internal heat generation.

II. EXPERIMENTAL APPARATUS AND PROCEDURE

A. EXPERIMENTAL APPARATUS

Convection Cell

The apparatus used in the present study was built by Emara [6] for his experiments on steady and transient convection with internal energy sources. He describes in detail its design and construction. Here, only a brief description of the apparatus and its instrumentation will be given.

The convection cell (Fig. 3) comprises three major components: the top plate, the bottom plate and the side walls. The fluid layer contained in the apparatus is 2.54 cm x 2.54 cm, and its depth is varied by changing spacers between the two horizontal plates. Two of the side walls of the cell are 1.27 cm thick Plexiglas sheets, while the other two were formed by electrodes for passing 60 Hz electric current through the aqueous electrolyte fluid layer. The bottom plate is a 1.9 cm thick Plexiglas sheet machined square to $\pm$ 0.0127 cm.

The convection chamber rests on a 1.27 cm thick Plexiglas sheet which acts as a foundation for the cell. In the bottom of this sheet, forty-one grooves were machined, each 0.317 cm wide and 1.27 cm apart for the length of the chamber. A 30 Ga nickel-chromium resistance heating wire was placed in these grooves. The purpose of the heater is to counter the downward heat flow and to maintain as nearly as possible a zero temperature gradient at the bottom of the layer. Preliminary calculations to approximate the heat loss from the lower surface indicated that the heater power required would be less than 0.7 W.

The electrodes in the side walls of the cell are copper-plated brass flats extending the entire length and depth of the cell. The dimensions of each electrode are 25.4 cm x 12.7 cm x 0.635 cm. Each is machined flat and polished by hand to a mirror finish.

The top plate is made of aluminum of 2.54 cm thickness. Eighteen cooling channels, each 1.778 cm wide and 1.905 cm deep, are machined in a flat double winding into the plate. The double winding of the cooling channels ensures that the plate can be maintained at a nearly uniform temperature since adjacent channels carry cooling water in opposite directions. The channeled plate is covered with a 0.635 cm thick aluminum plate, bolted to its open side. Finally a 0.0762 mm thick sheet of pressure sensitive Mylar was placed over the sides and bottom of the top plate to insulate it electrically from the current passing through the electrolyte.

Thermocouple wells, each 0.32 cm in diameter, are drilled into the top and bottom plates to within 0.128 cm of the surface in contact with

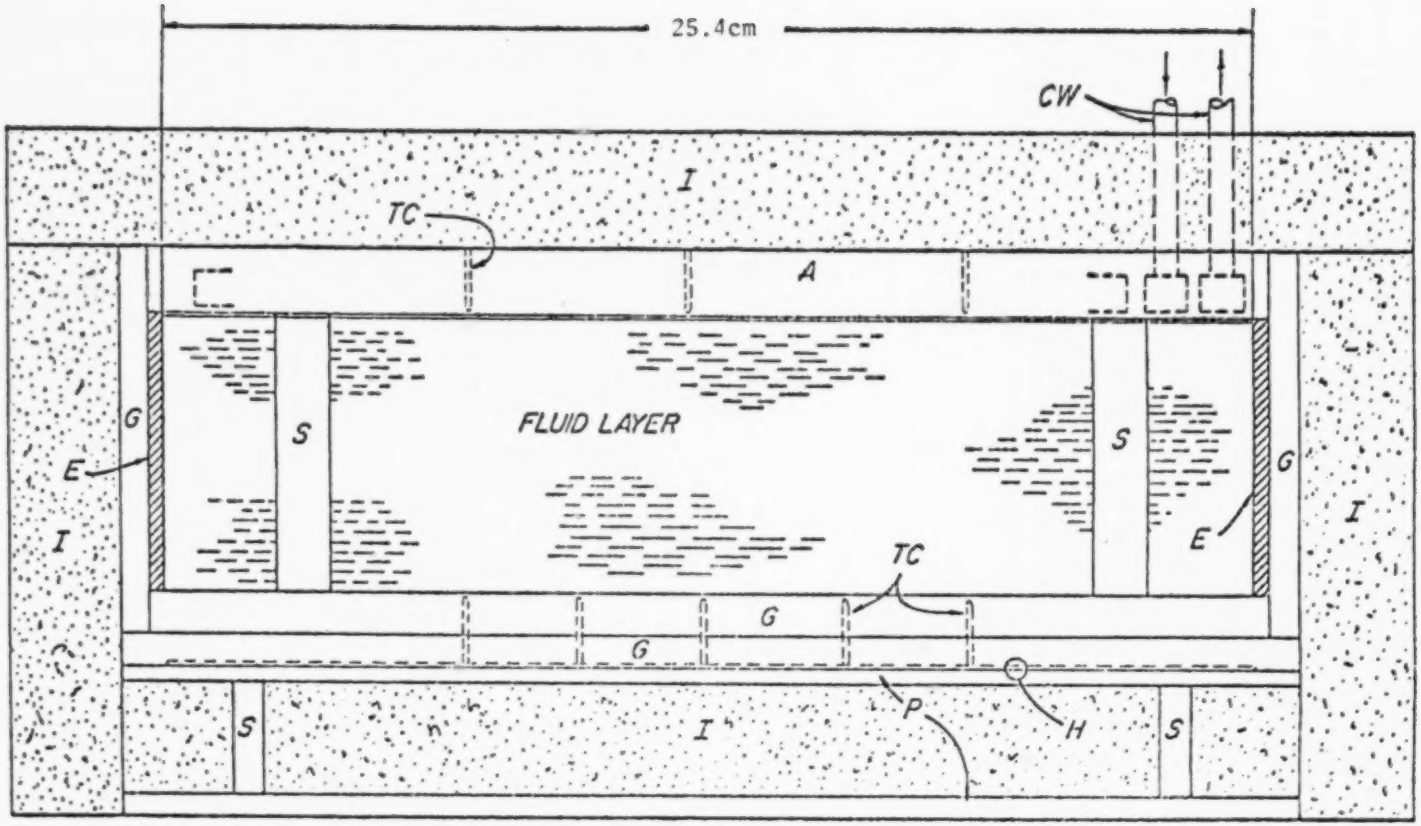

LEGEND

A	Aluminum	G	Plexiglas	P	Plywood
CW	Cooling Water	H	Resistance Heater	TC	Thermocouple Well
E	Electrodes	I	Insulation	S	Spacer

Figure 3. Detail View of Convection Cell

the fluid. The wells are spaced uniformly around the plate to obtain an average measurement. All thermocouples are painted with insulating varnish. Thermocouples in the bottom plate are secured in their wells with epoxy cement; thermocouples in the top plate are secured in their wells with copper oxide cement.

When the plate is placed into the convection chamber, it rests on spacers which are machined from 2.54 cm diameter Plexiglas rods. The spacers are made to a specified length to within $\pm$ 0.00127 cm. The top, bottom and side walls of the convection chamber are insulated with styrofoam insulation board, 5.08 cm thick. Two removable rectangular cuts were made on two sides of the insulation material, thus allowing inspection of the layer through the two Plexiglas side walls. The entire chamber rests on a triangular stand for leveling purposes. Leveling is accomplished by adjusting a screw at each of the three corners of the stand.

Instrumentation

A schematic of the convection cell and instrumentation is shown in Fig. 4.

For steady-state heat transfer measurements as well as transient experiments, it is necessary to measure the temperature difference across the layer with high precision. Therefore, all thermocouples are monitored by a Leeds and Northrup Model 8686 milivolt potentiometer. Readings are accurate to $\pm$ 1μv. For measurements made in this study, this would be equivalent to $\pm$ 0.019°C.

Iron-constantan thermocouples have been used for temperature measurements within the convection chamber and for recording the transient temperature at the bottom of the convection chamber. One thermocouple is selected as a reference and all others compared to the reference output at the ice point and at the boiling point of water. The reference is then calibrated against a high precision mercury thermometer. No resolvable difference in converted thermocouple output and temperature was detected. For measurements of the temperature difference across the layer, five thermocouples each in the top and bottom plates were connected in parallel. The output of each parallel circuit is determined relative to a reference at 0°C. The difference in the two millivolt outputs determined in this way gives a reliable measurement of the temperature difference across the layer. One thermocouple was placed in the bottom plate 0.128 cm from its surface for recording the transient behavior of temperature at the bottom of the fluid layer.

The thermocouple arrangement for determining the heat flux through the bottom plate is a differencing thermopile using ten thermocouples. Five thermocouples are spaced across the bottom plate at 0.128 cm from its surface, and another five thermocouples are spaced at 1.398 cm from the bottom surface. Thus, the output of the thermocouple can be

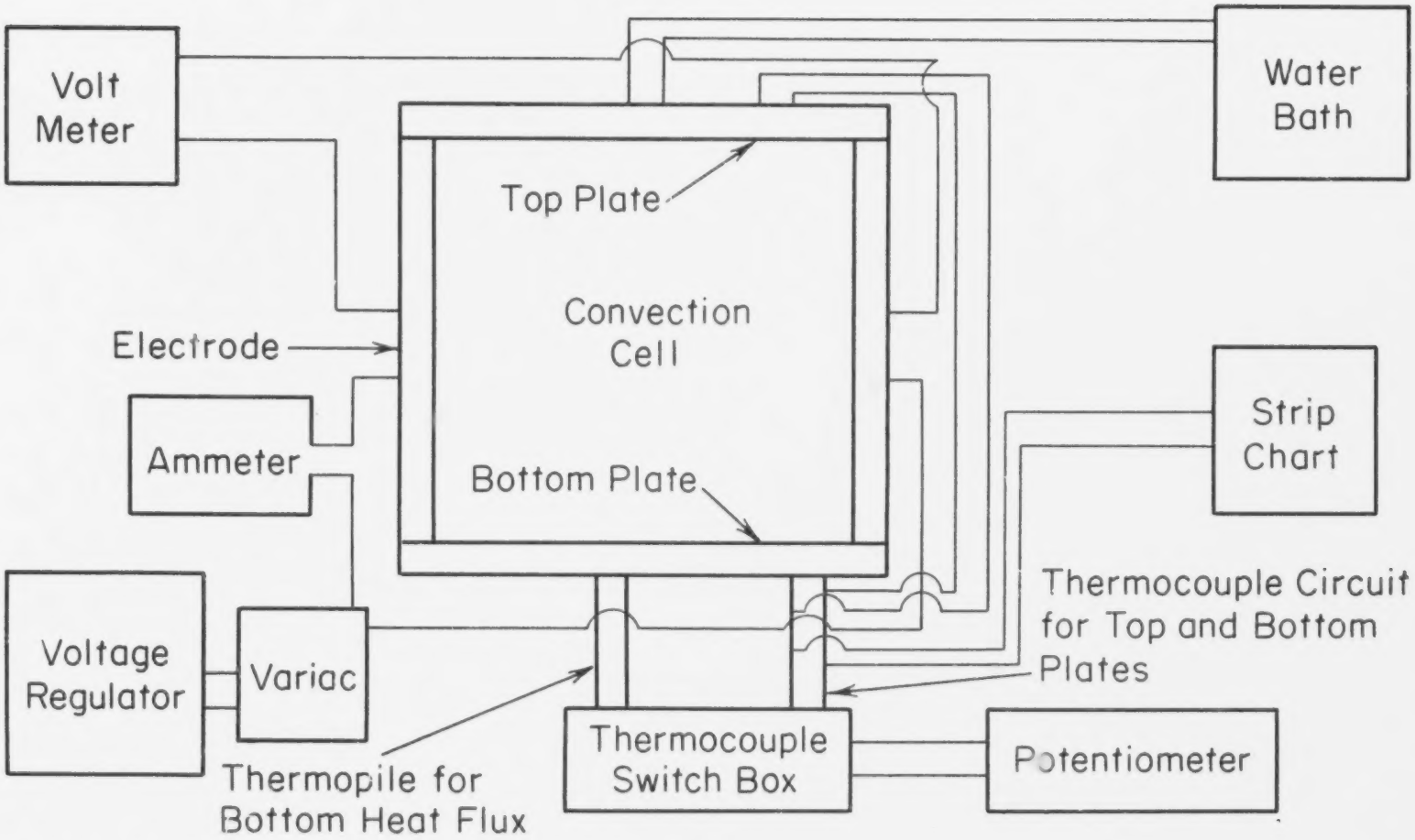

Figure 4. Schematic Diagram of Apparatus and Instrumentation

interpreted as a measure of the heat flux across the bottom plate.

A strip chart recorder is used to record the temperature history at the bottom of the fluid layer. The output of the thermocouple is first amplified by proper adjustment of zero off-set and span adjustment of the recorder. The published accuracy of the recorder is ± 0.25% of span or ± 3.5 μv (whichever is greater), and its response time is less than 0.3 s full scale, which is sufficient for the thermal transients being measured in this study.

Energy generation in the fluid layer is accomplished by Joule heating in the electrochemical all formed by the two copper plated electrodes and the electrolyte of dilute aqueous copper sulfate (concentration of 0.4% copper sulfate by weight) in the layer. The output of a voltage regulator is connected to a Variac so that regulation of power input to the convection chamber could be achieved. Power consumed is measured by obtaining the current and voltage independently. An ammeter with an accuracy of 0.5% of the full scale reading and a digital multimeter with the same accuracy are used for this purpose.

A constant temperature bath is used to supply cooling water to the constant temperature top plate. Supply water temperature could be controlled within ± 0.05°C.

B. EXPERIMENTAL PROCEDURE

Initially, all reference thermocouples are placed in an ice-point reference bath, and the interior of the convection chamber is cleaned with demineralized water. The electrode surfaces are polished with copper polish and then wiped clean with acetone to remove any residue. Fine horizontal alignment is accomplished by placing a level with a sensitivity of 0.0416 cm/m on the base and adjustment of the legs on the triangular stand. The four Plexiglas spacers of a desired height, cleaned with acetone are positioned at each corner around the cell to support the top plate. The layer is then filled with aqueous solution of copper sulfate. The copper sulfate solution is prepared using demineralized, degassed water. Filling is done slowly to prevent entrapment of air in the layer as the fluid was added. When the layer is viewed through the window on the side, it is possible to determine when the layer is just filled.

After the fluid layer has been prepared, the top plate is very slowly lowered onto the convection cell until it comes into contact with the fluid and the spacers. The plate is then tilted slightly at an angle to let trapped air bubbles escape. The top plate is then allowed to settle down flat on top of the spacers.

Before applying a step increase in power to the fluid layer, the initial temperatures of the top plate, fluid layer and bottom plate are brought to exactly the same value. Since most of the experiments are

transitions from one state of steady convection to another following a step-change in the power input to the layer; the above procedure does not have to be repeated for most of the experiments.

During the course of the study it was found very important to keep the thermal boundary conditions on the fluid layer as close as possible to the ideal conditions during the transition period. This is achieved by monitoring the heat flux through the bottom plate as a function of time on the strip chart recorder, and making the necessary adjustment in the voltage input to the guard/heater. Furthermore, periodic adjustments to the constant temperature bath were made on the flow rate and temperature setting in order to maintain the top plate at constant temperature. Once the steady-state is reached, temperature data are recorded and a new step-change in the power input to the layer is applied. The above procedure is then repeated.

The error in determining the temperature difference and the overall errors in recording the data as described are discussed in Appendix C.

III. PRESENTATION AND DISCUSSION OF RESULTS

A. STEADY STATE HEAT TRANSFER

The Nusselt number at the upper surface of the fluid layer is defined using the depth of the fluid layer, L, as the characteristic length dimension and the difference in temperature between top and bottom plates as the characteristic temperature difference. Thus, the Nusselt number in terms of the power dissipated within the layer becomes,

$$Nu_1 = \frac{(P - P_L)L}{kA(T_o - T_1)} \tag{20}$$

The Rayleigh number is computed as defined in Eq. (2).

The thermophysical properties of the aqueous copper sulfate solution which served as the fluid medium in the convection cell are necessary for calculation of the Rayleigh number, Nusselt number and Fourier number. However, sufficient data for the concentration dependence of such a solution does not exist and therefore the thermophysical property values of water are used as a function of temperature alone. The thermophysical properties of the fluid appearing in Nu_1, Ra and Fo are, in all cases, evaluated at the bottom plate temperature. A summary of the thermophysical properties of water are given in Table A-1.

Experimental data for steady state heat transfer are given for each run in tabular form in Table B-1. A graphical presentation of measured Nusselt numbers is given in Fig. 5 in conjunction with the correlation given by Kulacki and Emara [9]. Present results are in good agreement with those of Kulacki and Emara. The ratio of the maximum temperature difference across the fluid layer and the maximum possible temperature difference for pure conduction model is plotted against the Rayleigh number in Fig. 6. For the range of Rayleigh number shown in Fig. 6, $10^7 \leq Ra \leq 10^{10}$, it is found that the maximum temperature difference, varies between 3% and 15% of the pure conduction temperature difference, $(HL^2/2k)$.

B. TRANSIENT CONVECTION

Transient temperatures in the present study were measured with a thermocouple placed in the bottom plate 0.128 cm from its surface. In the transient experiments of Kulacki and Emara [9], the temperature was recorded by a glass encased thermocouple inserted into the center of the cell through a hole in the top plate. In the present study, this method of temperature recording was discarded due to electrical current leakage from the fluid to the top plate. The present method of recording temperature development is estimated to introduce a time lag in response of up to 80% of the measured time compared to Kulacki and Emara's

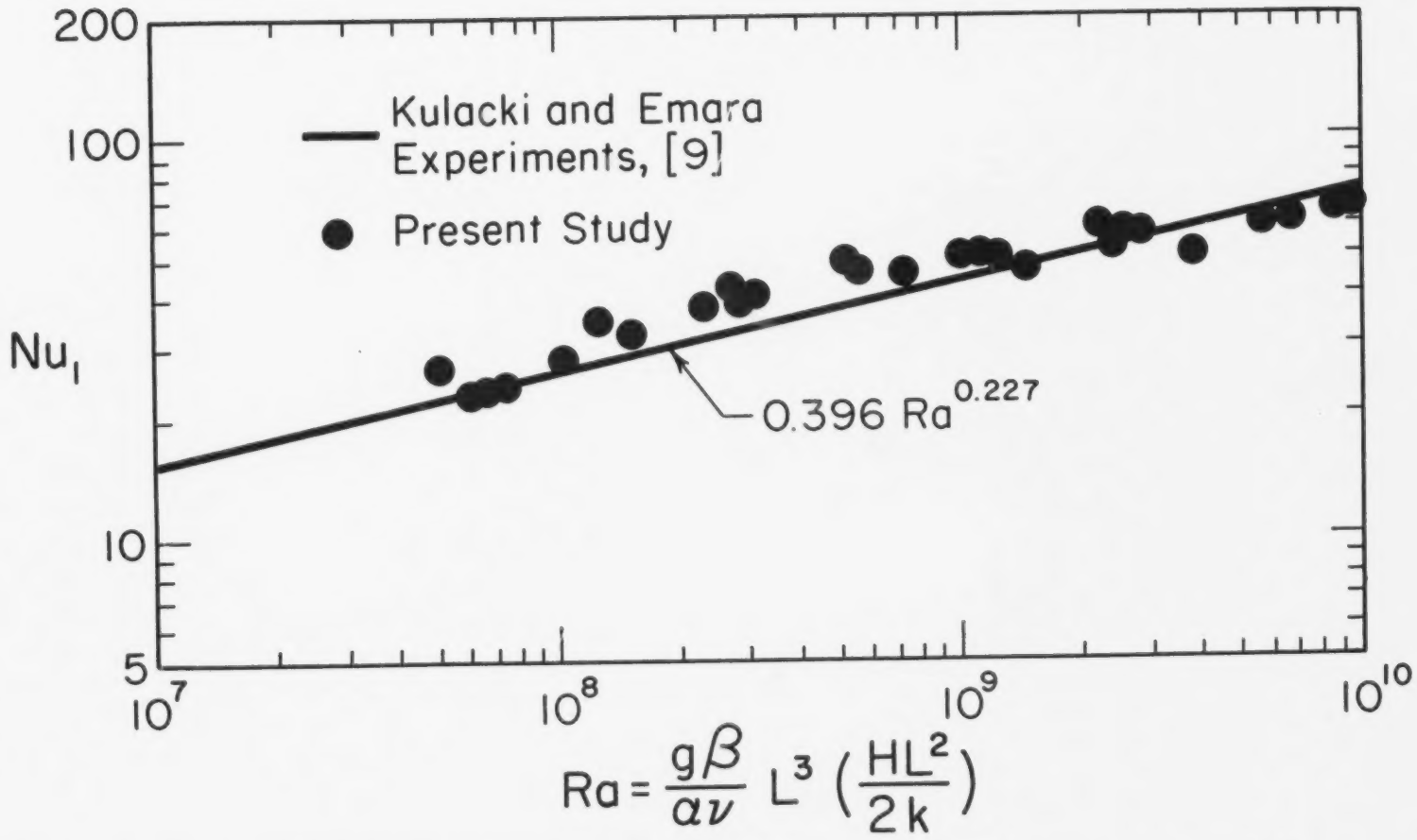

Figure 5. Steady-State Nusselt Numbers Obtained from Asymptotic Values of the Temperature Difference Following a Step Change in Rayleigh Number

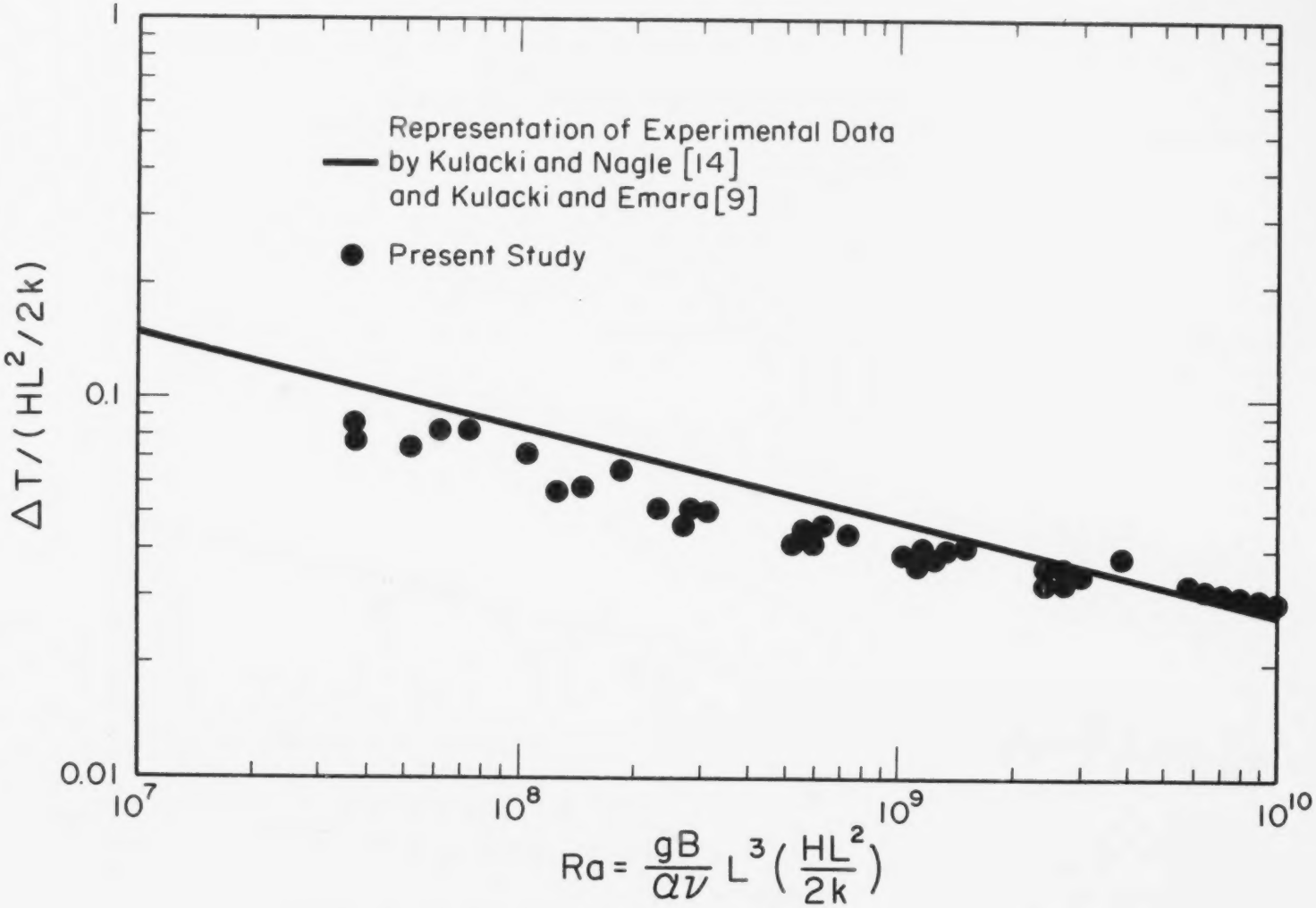

Figure 6. Steady-State Non-Dimensional Temperature Difference Data

measurements. A typical thermocouple response versus time, and the definition of maximum time, t_{max}, and the pseudo first-order time constant, t_{σ}, for the maximum temperature difference within the layer are given in Fig. 7. When the recorded temperature was within 2% of the apparent steady state value, that time was taken as the value in computing the layer Fourier number.

The experimental runs in the present study include step increases in the Rayleigh number (i.e., heating-up of the layer, $Ra_I = 0$), step decreases in the Rayleigh number (i.e., cooling-off of the layer without internal heat sources, $Ra_F = 0$), and the step change in the Rayleigh number for transition from one state of steady convection to another (i.e., $Ra_F > 0$, $Ra_I > 0$). Experimental data for transient convection are given for each run in tabular form in Tables B-2, B-3, B-4 and B-5. The experimental data obtained for the transition from one state of steady convection to another following a step change in the internal heat generation indicate that the time required for this transition is a function of the step change in the Rayleigh number and the initial dimensionless core temperature, θ_{co_I}. The theoretical analysis performed by Cheung [5] based on the boundary layer approximation confirms this. Graphical illustration of this point, is given in Figs. 8 and 9. Cheung's prediction for the maximum time required for the transition from one state of steady convection following a step change in the internal heat generation is obtained from the numerical solution of Eq. (16). It should be noted that the numerical solution of Eq. (16) converges very rapidly initially but, thereafter, converges very slowly to the final steady state value. For large times, approximately a 40% increase in the Fourier number introduces 0.1% change in the temperature difference across the fluid layer.

The initial dimensionless core temperature acts as a parameter in the plot of step change in the Rayleigh number versus the Fourier number in Figs. 8 and 9. This can be eliminated by normalizing the dimensionless time through dividing it by the initial dimensionless temperature for a given step change in the Rayleigh number. The normalized Fourier number versus the step change in the Rayleigh number is shown in Figs. 10 and 11, for developing and the decaying flows. The present results for developing flow are in good agreement with Cheung's prediction. In the case of decaying flow, the results of the present study are in fairly good agreement with the maximum Fourier number predicted by Cheung.

The step change in the Rayleigh number can be represented either in the form Ra_F/Ra_I, or by $|Ra_F - Ra_I| = |\Delta Ra|$. In the previous figures, the first form of representing step change in the Rayleigh number is used. Kulacki and Emara's [9] experiments are restricted to complete decay (i.e., $Ra_F = 0$) and heating-up of the layer (i.e., $Ra_I = 0$). Therefore, in the presentation of their results, the step change in the Rayleigh number is given in terms of $|\Delta Ra|$.

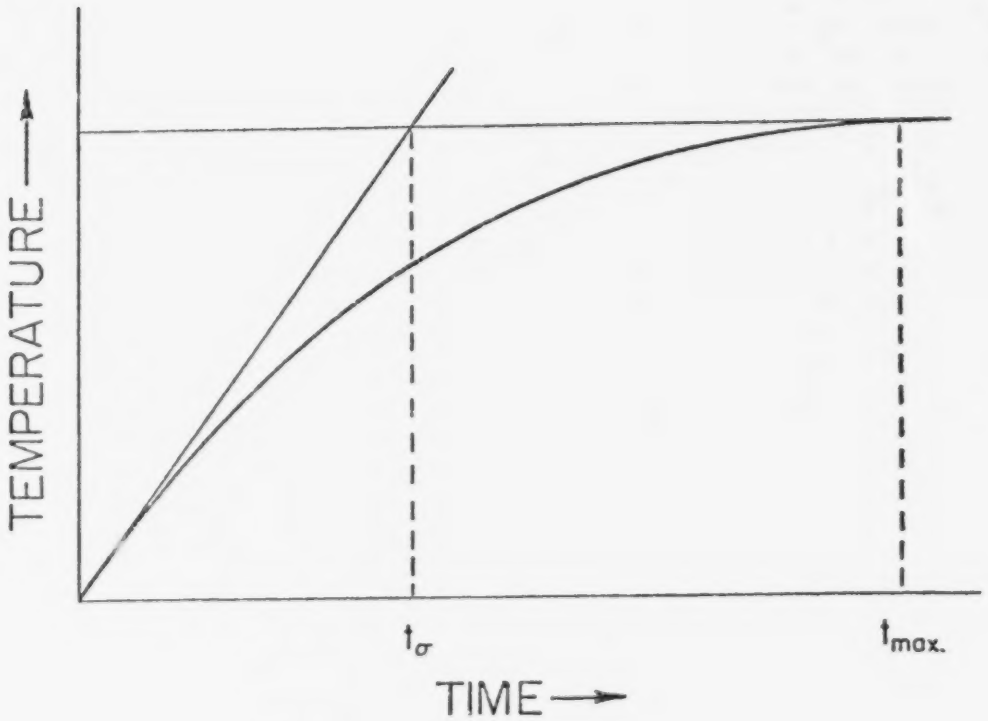

Figure 7. Typical Thermocouple Response versus Time and Definition of t_σ and t_{max}

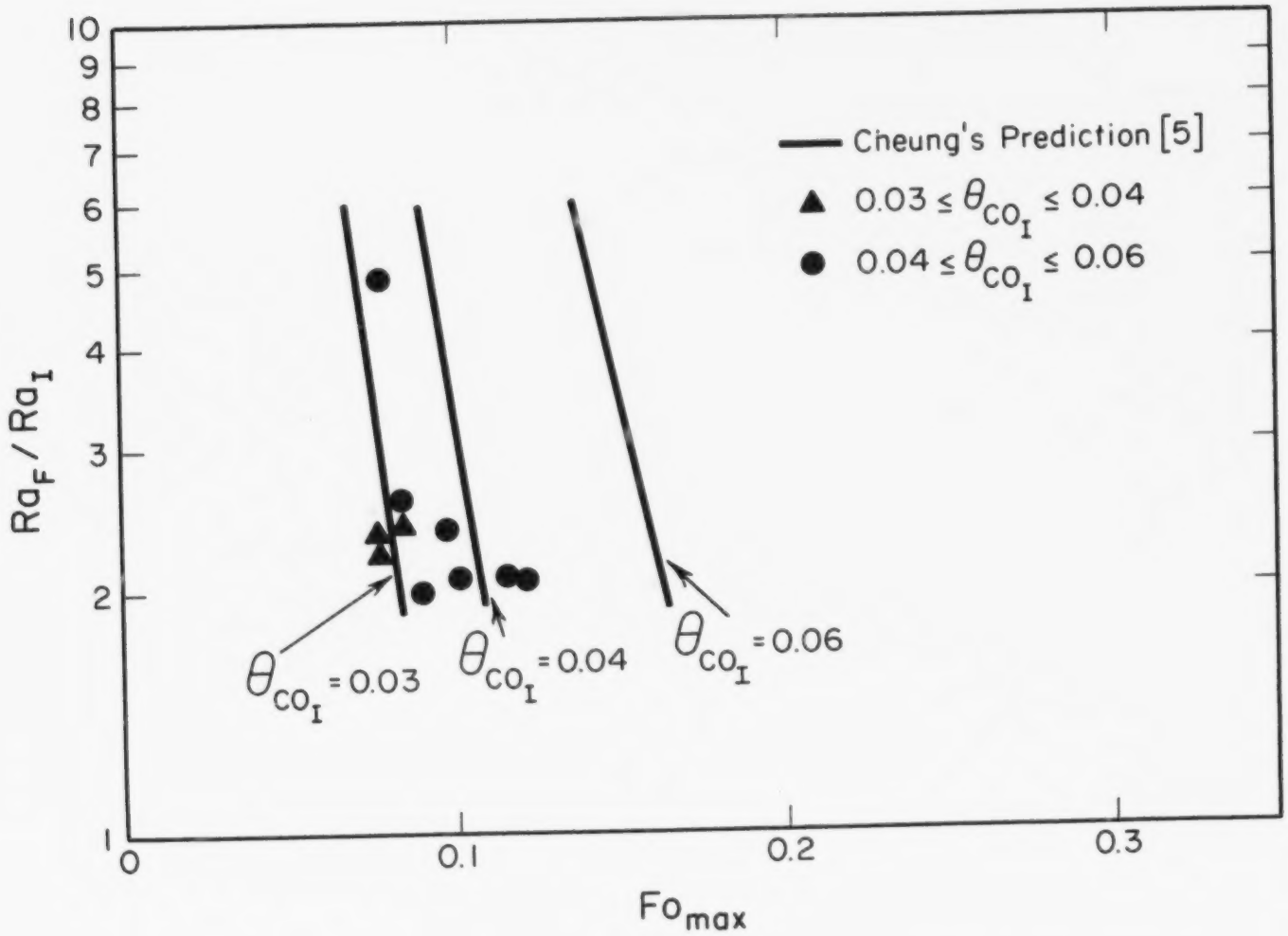

Figure 8. Step Change in the Rayleigh Number versus the Fourier Number with the Initial Dimensionless Core Temperature as the Parameter in the Developing Flow

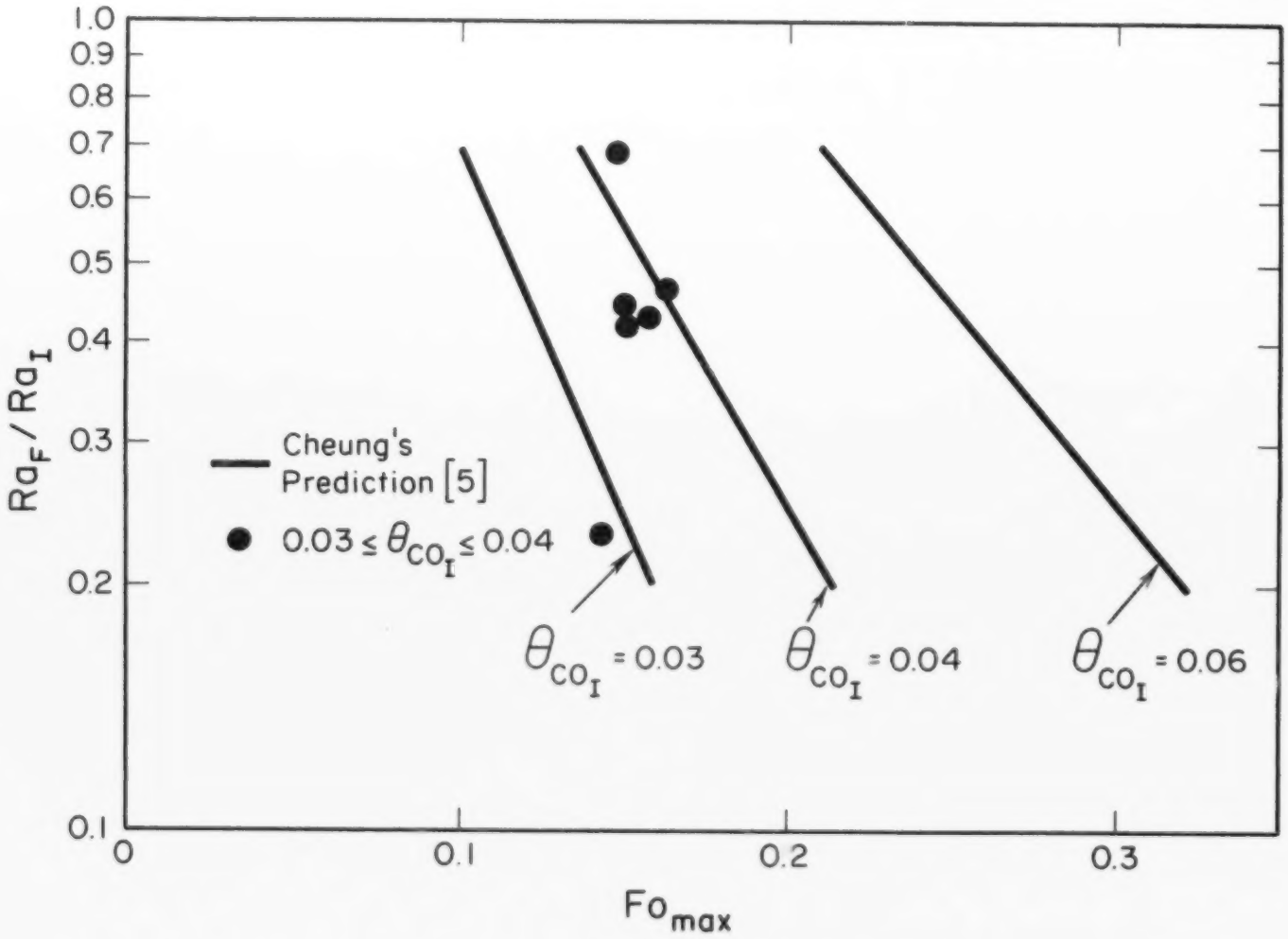

Figure 9. Step Change in the Rayleigh Number versus the Fourier Number with the Initial Dimensionless Core Temperature as the Parameter in the Decaying Flow.

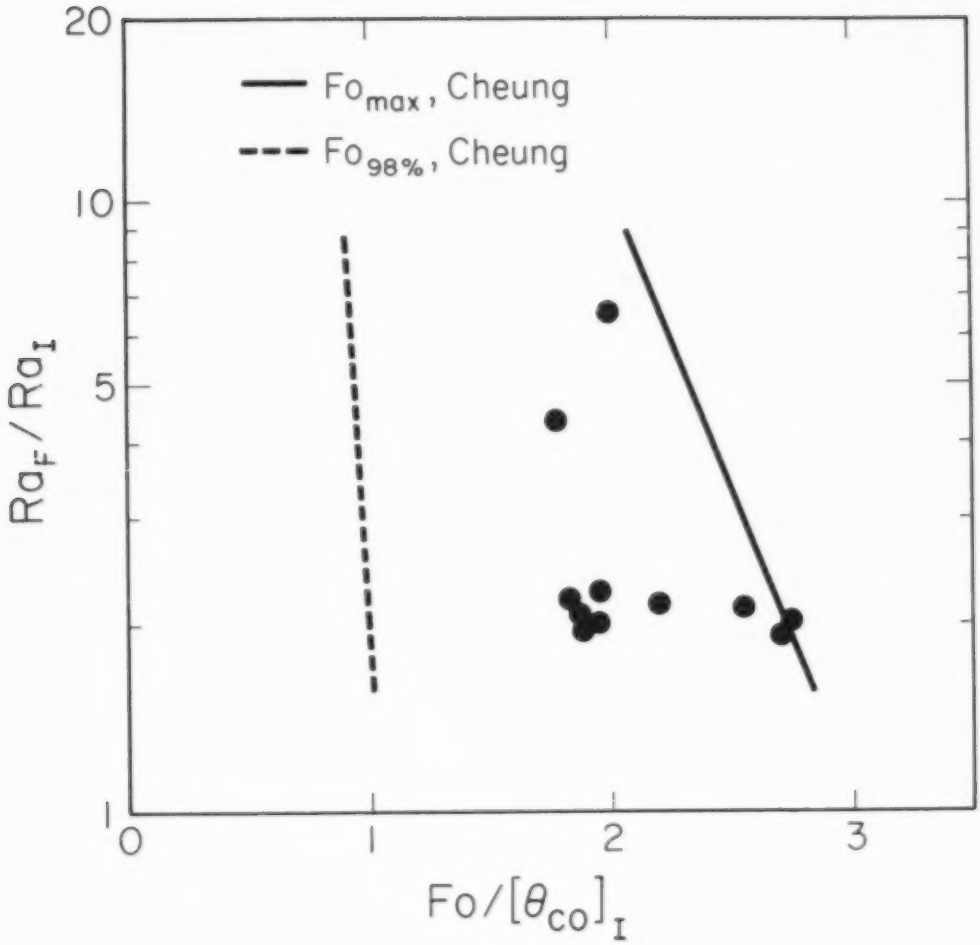

Figure 10. Fourier Numbers for Developing Flow Compared to the Predictions of Cheung

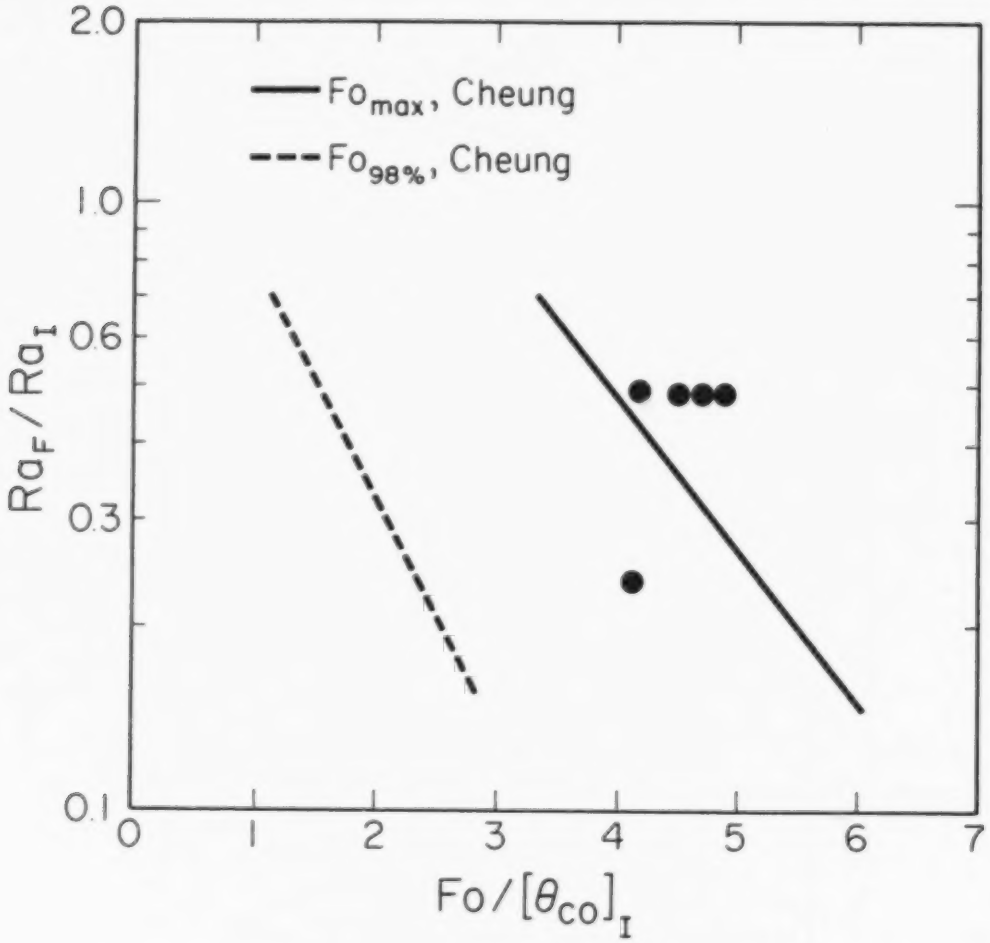

Figure 11. Fourier Numbers for Decaying Flow Compared to the Predictions of Cheung

In order to graphically illustrate the step increase in the Rayleigh number, $|\Delta Ra|$, for transition from one state of steady convection to another versus the Fourier number, it is necessary to have the initial dimensionless core temperature as a parameter. A family of curves representing step increase in the Rayleigh number versus the Fourier number are shown in Fig. 12, where the initial Rayleigh number is given as the parameter. The interchange of dimensionless core temperature and the Rayleigh number is justified, since there is a direct relationship between the two (Fig. 6).

In the case of decaying flow, the parameter which distinguishes between complete decay and the transition from one state of steady convection to another is the final dimensionless temperature, rather than the initial temperature, as is in the case of developing flow. A family of curves representing a step decrease in the Rayleigh number versus the Fourier number is presented in Fig. 13, where the final Rayleigh number serves as a parameter.

The results of the present study for the case of step increase in the Rayleigh number, $|\Delta Ra|$, versus the Fourier number, Fo, are presented in Fig. 14 in conjunction with correlation (for $Ra_I = 0$) given by Kulacki and Emara [9]. The results of the present study for $Ra_I = 0$, are in very good agreement with the correlation reported by Kulacki and Emara. Experimental data representing the step increase in Rayleigh number with $Ra_I > 0$, indicates that a shorter time is required for the completion of the transition from one state of steady convection to another, compared to the time for transition from a motionless state to a state of steady convection for the same $|\Delta Ra|$. This behavior is in accordance with the existence of a family of curves as presented in Fig. 12.

The graphical presentation of results of the present study for the case of step decrease in the Rayleigh number versus the Fourier number is given in Fig. 15 in conjunction with the correlation (for $Ra_F = 0$) given by Kulacki and Emara [9]. The experimental data of the present study for $Ra_F = 0$, indicates that a longer time is required for the complete decay compared to the time predicted by correlation reported by Kulacki and Emara. Furthermore, the experimental data of the present study indicates that, for the same $|\Delta Ra|$, a shorter time is required for transition from one state of steady convection to another rather than that of a complete decay. This behavior is as expected from the curves illustrated in Fig. 13.

As previously discussed, the experimental data of the present study and the theoretical analysis of Cheung [5] confirms the existence of a family of curves for the step change in Rayleigh number, $|\Delta Ra|$, as a function of the Fourier number with Ra_I and Ra_F as parameters for developing and decaying flows respectively. Unfortunately, numerous experimental runs are required to establish these curves experimentally. However, appropriate normalization of the dimensionless parameters, particularly, $|\Delta Ka|$, permits a smaller number of experiments to meet the

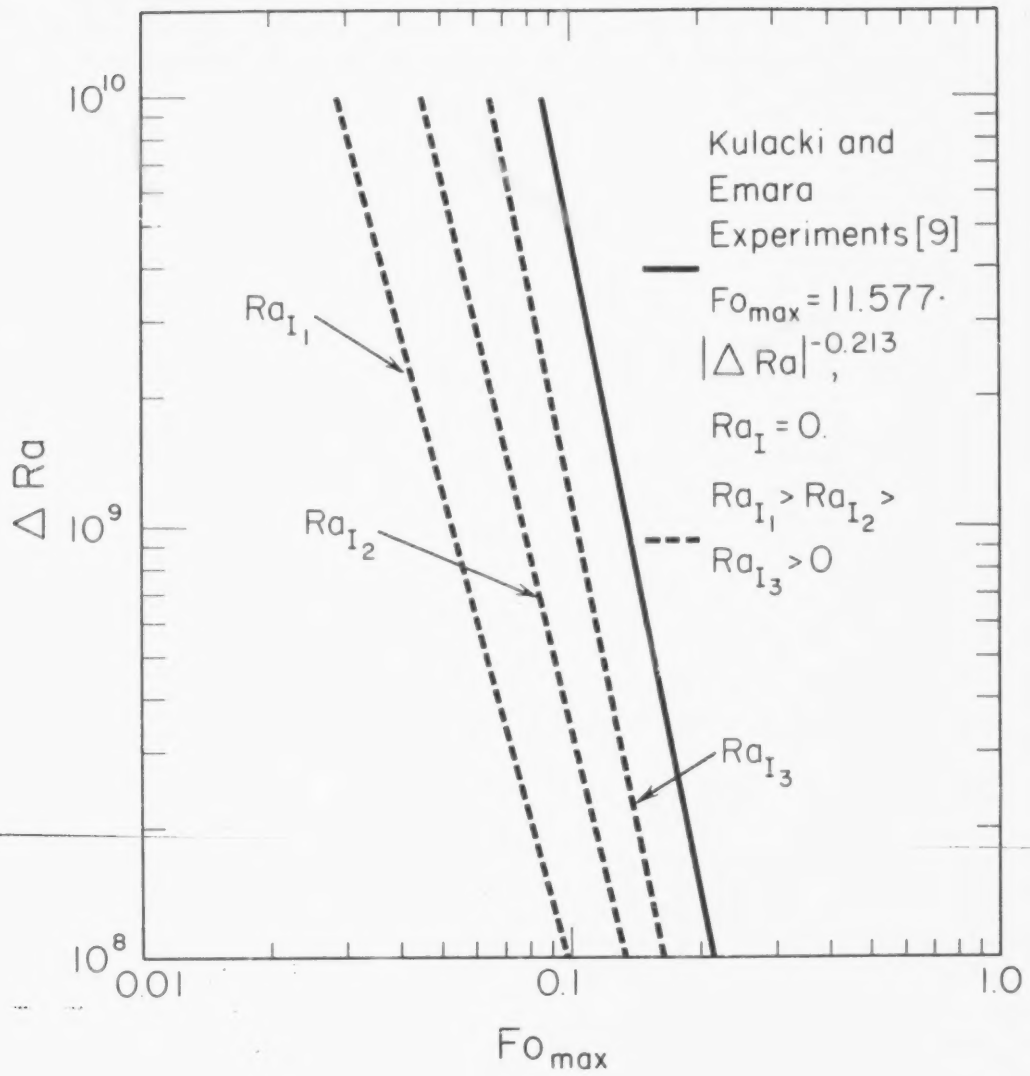

Figure 12. Family of Curves Representing Step Increase in the Rayleigh Number versus the Fourier Number

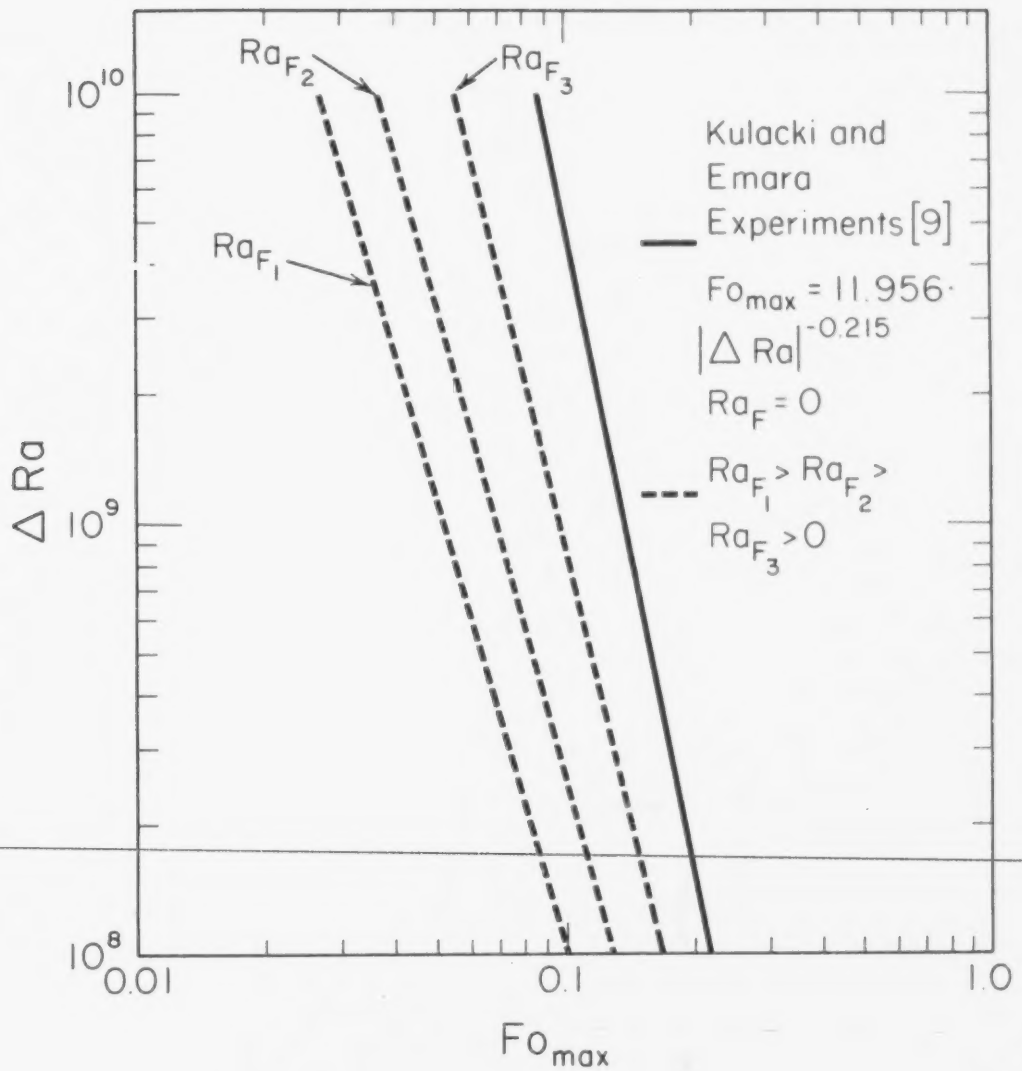

Figure 13. Family of Curves Representing Step Decrease in the Rayleigh Number versus the Fourier Number

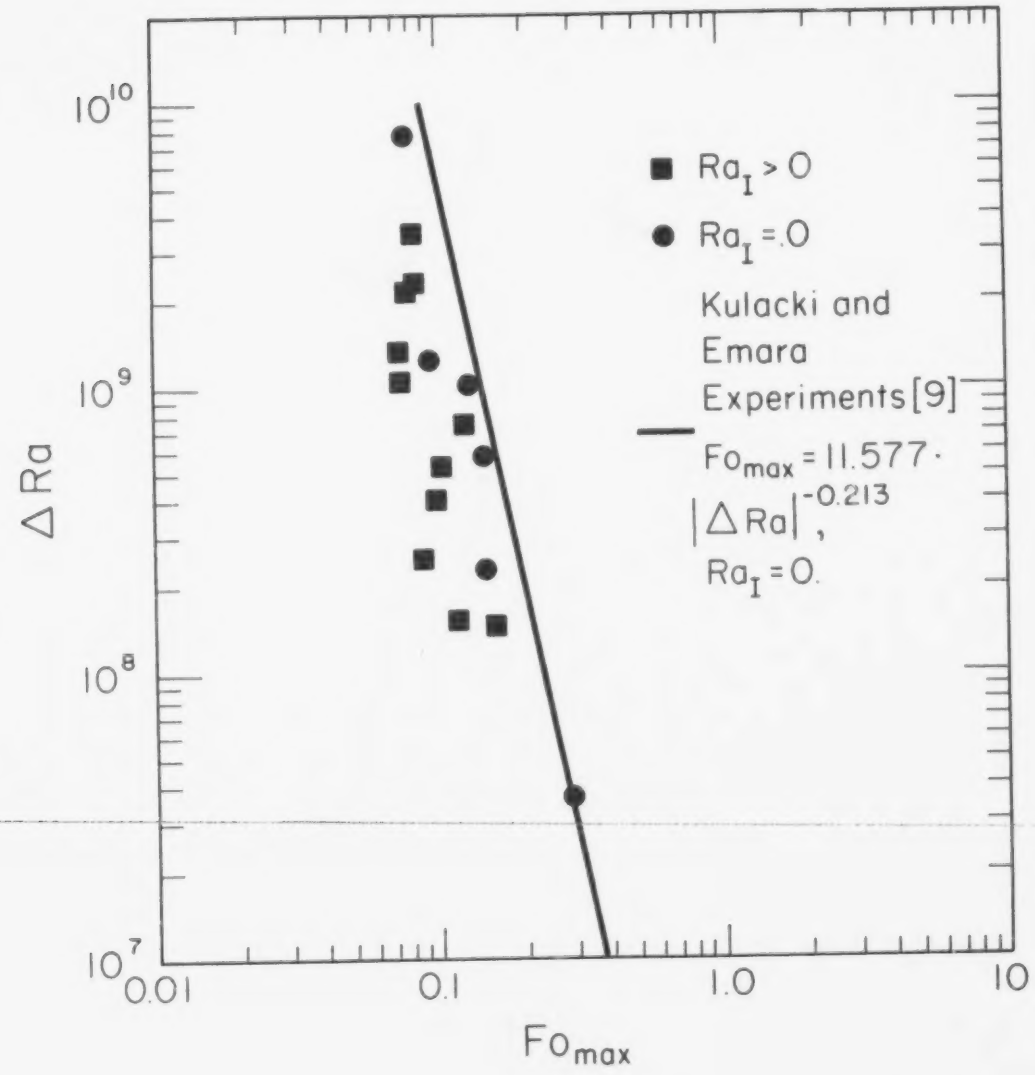

Figure 14. Step Increase in the Rayleigh Number versus Dimensionless Time

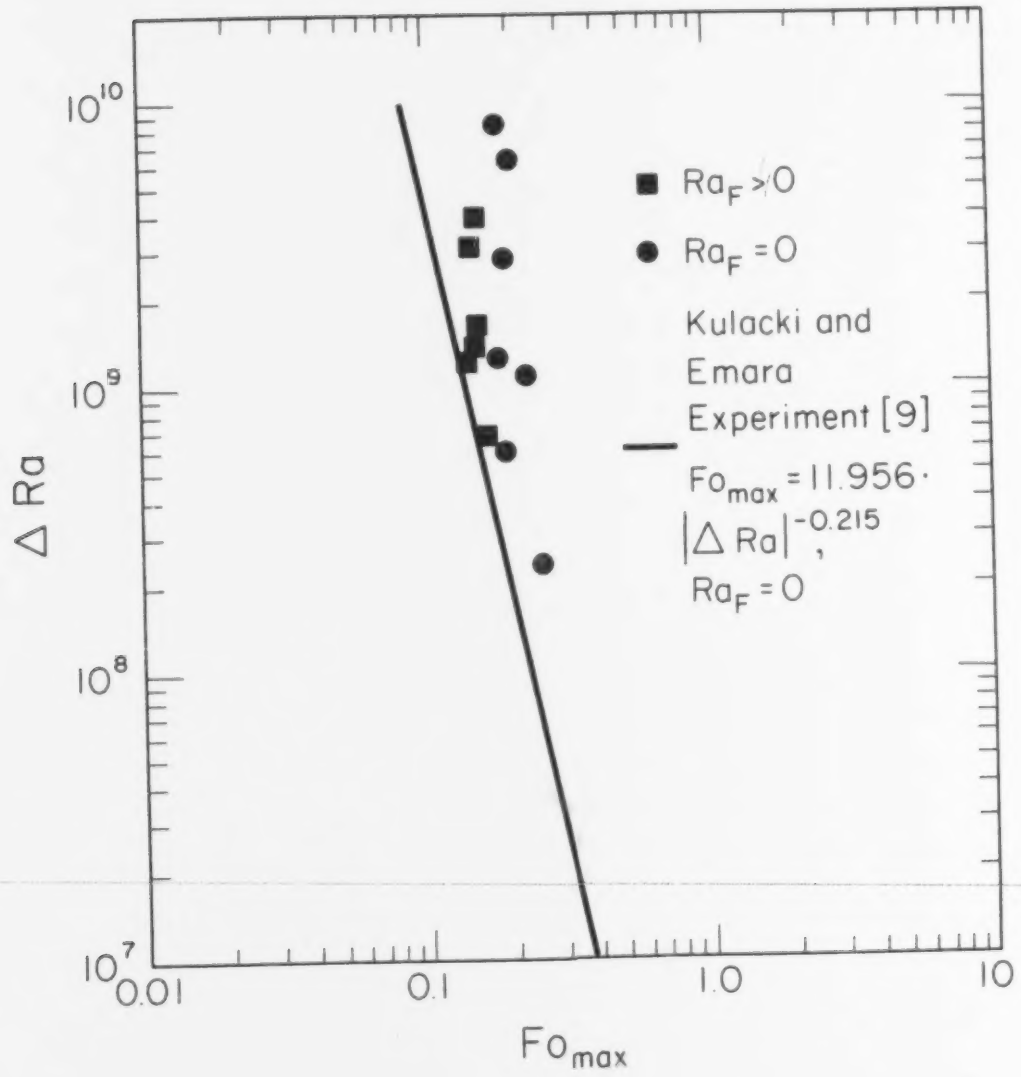

Figure 15. Step Decrease in the Rayleigh Number versus Dimensionless Time

same objective.

Normalization of the step increase in the Rayleigh number, ΔRa, is achieved by dividing the ΔRa, by the initial dimensionless core temperature, θ_{co_I}, which is the parameter that distinguishes between the heating up of the layer with $Ra_I = 0$, and the transition from one state of steady convection to another, (i.e., $Ra_I > 0$). This method of normalization is valid for $Ra_I = 0$, since the initial dimensionless core temperature has the value of unity in this case. Therefore, it is justified to compare the normalized step change in the Rayleigh number, $|\Delta Ra|/\theta_{co_I}$, and its corresponding Fourier number with the correlation reported by Kulacki and Emara [9], with $\theta_{co_I} = 1$.

The normalized step increase in the Rayleigh number, $\frac{\Delta Ra}{\theta_{co_I}}$, as a function of the Fourier number, is shown in Fig. 16 in conjunction with the correlation given by Kulacki and Emara [9], with $\theta_{co_I} = 1$, and the predictions of Cheung [5]. The predictions of Cheung give the range of Fourier number where the maximum temperature difference is within two percent of the final steady state value, i.e., $Fo_{98\%} \leq Fo \leq Fo_{max}$. The results of the present study and the theoretical predictions by Cheung and the correlation reported by Kulacki and Emara are in a satisfactory agreement for the case of developing flow.

In the case of decaying flow, the normalization is achieved by dividing the step change in the Rayleigh number, $|\Delta Ra|$, by the final dimensionless core temperature, θ_{co_F}. The normalization in this case is done through the final dimensionless core temperature, θ_{co_F}, since it is the parameter which distinguishes between complete decay and the transition from one state of steady convection to another. This method of normalization is valid in the case of complete decay where the value of final dimensionless core temperature is unity.

The normalized step decrease in the Rayleigh number, $\frac{\Delta Ra}{\theta_{co_F}}$, versus the Fourier number are presented in Fig. 17. The correlation given by Kulacki and Emara [9], with $\theta_{co_F} = 1$ and the predictions of Cheung [5] are also shown in Fig. 17. Predictions of Cheung give the range of Fourier number where the temperature difference across the layer is within two percent of the final steady-state value. The results of the present study indicate that a longer time is required for the complete decay compared to the time obtained from the correlation reported by Kulacki and Emara. Cheung's predictions are in good agreement with the results of the present study for complete decay. Moreover, the experimental data of the present study are in fairly good agreement with maximum Fourier number predicted by Cheung's boundary layer analysis for transition from one state of steady convection to another. It

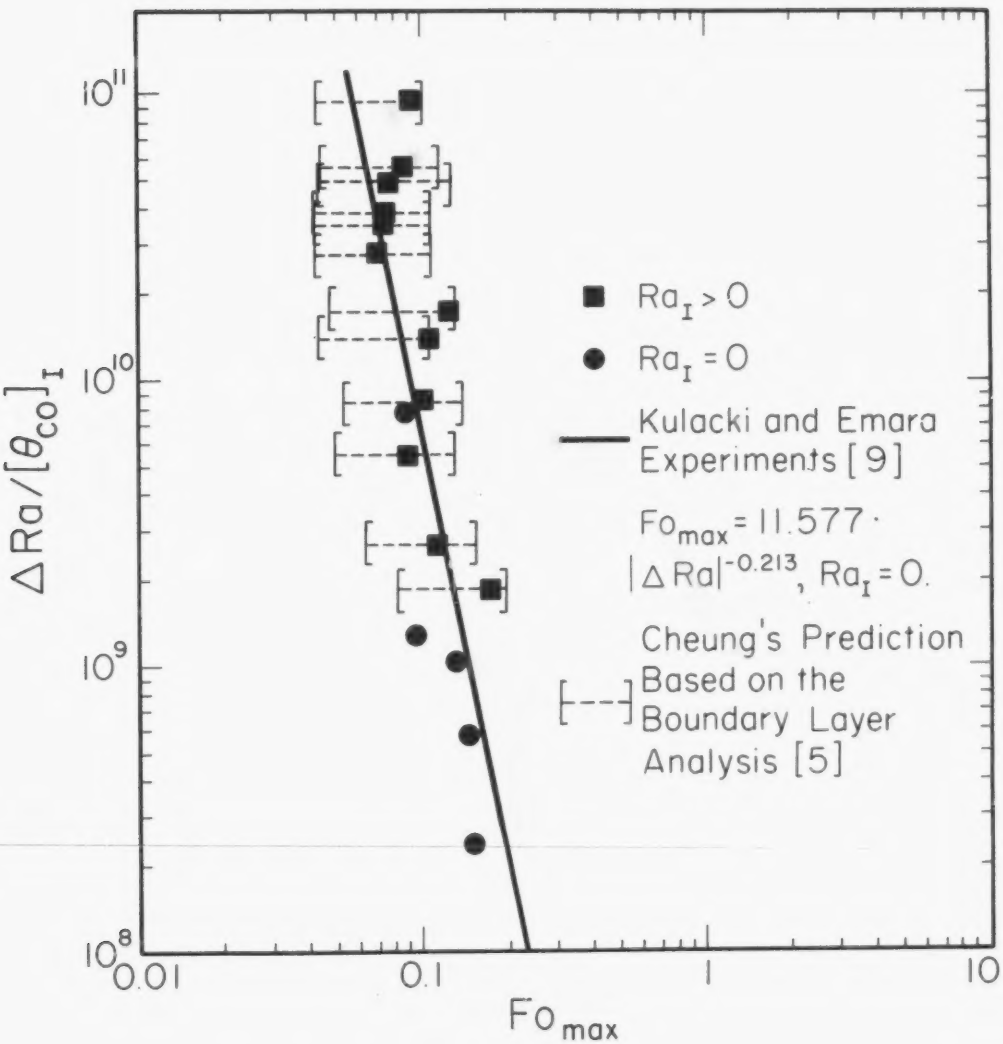

Figure 16. Normalized Step Increase in the Rayleigh Number versus Dimensionless Time. Predictions of Cheung[5] Give the Range of Fourier Number Where the Maximum Temperature Difference is Within Two Percent of the Final Steady-State Value (i.e., $Fo_{98\%} \leq Fo \leq Fo_{max}$)

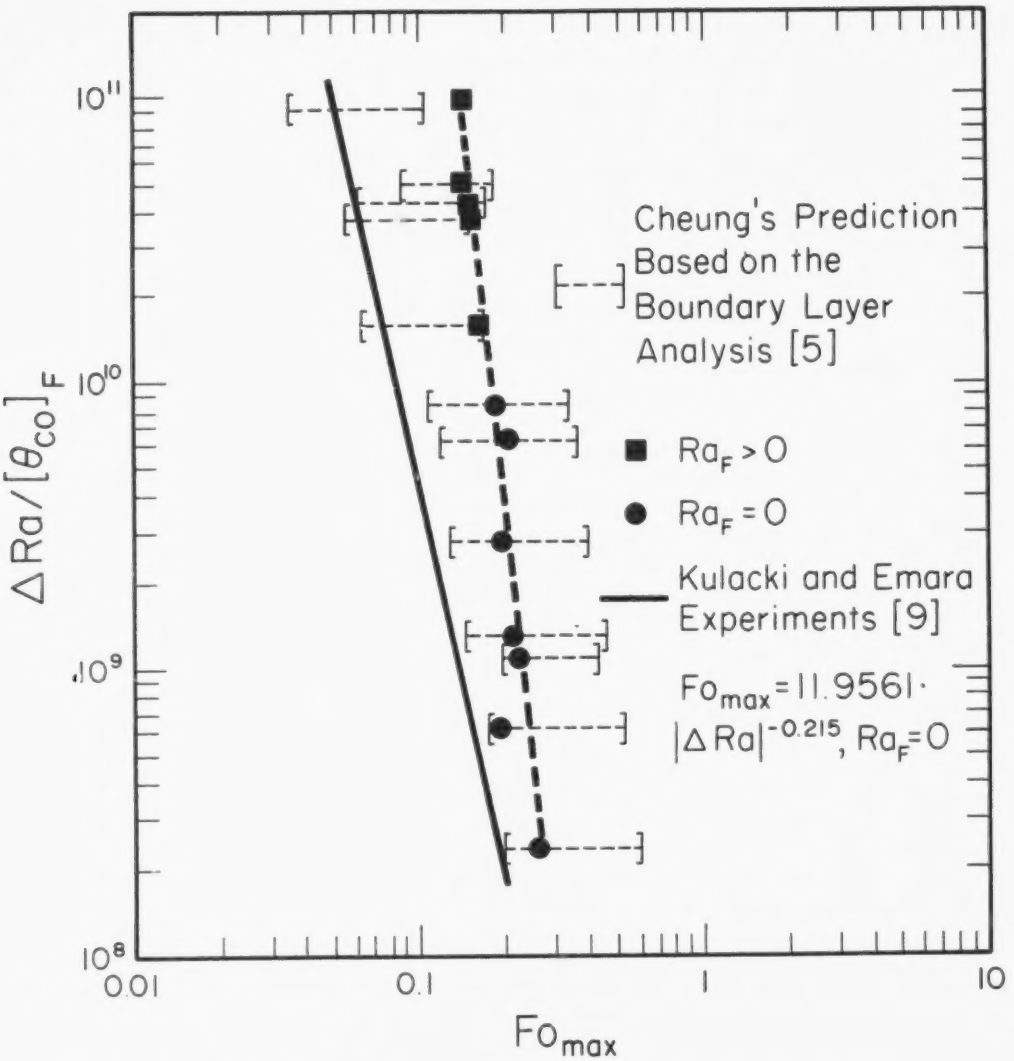

Figure 17. Normalized Step Decrease in the Rayleigh Number versus Dimensionless Time. Predictions of Cheung [5] Give the Range of Fourier Number Where the Minimum Temperature Difference is Within Two Percent of the Final Steady-State Value (i.e., $Fo_{98\%} \leq Fo \leq Fo_{max}$)

should be noted that, for the same step change in Rayleigh number, a longer time is required for decaying flow than that of a developing flow. This is confirmed through the results of the present study and the results obtained from the boundary layer analysis.

A plot of the experimental data of the present study on logarithmic coordinates, indicates that an equation of the form

$$Fo = \text{Constant} \left(\frac{\Delta Ra}{\theta_{co_I}} \right)^n \tag{21}$$

for developing flow and,

$$Fo = \text{Constant} \left(\frac{\Delta Ra}{\theta_{co_F}} \right)^n \tag{22}$$

for decaying flow adequately describe the trend in the data for the range of Rayleigh number under consideration in the present study, i.e., $10^7 < Ra < 10^{10}$ (see Figs. 16 and 17).

The normalized step <u>decrease</u> in the Rayleigh number, $\frac{\Delta Ra}{\theta_{co_F}}$, is correlated with the maximum Fourier number, Fo_{max}, via a linear regression of ln(Fo) on ln ($|\Delta Ra|/\theta_{co_F}$) by

$$Fo_{max,\ cooling} = 1.046 \left(\frac{|\Delta Ra|}{\theta_{co_F}} \right)^{-0.0778} \tag{23}$$

Equation 23 is presented in graphical form in Fig. 18 in conjunction with correlation given by Kulacki and Emara [9] for complete decay, and prediction of Cheung [5] for complete decay. Cheung's prediction is the time required for the temperature difference across the layer to reach to within two percent of the final steady-state value, i.e., Fo_{ss}. Cheung's prediction indicates that a longer time is required for the completion of the decay of the flow compared to the time, Fo_{max}, indicated by the correlation reported by Kulacki and Emara.

Normalized step <u>increases</u> in the Rayleigh number, $\frac{\Delta Ra}{\theta_{co_I}}$, versus the Fourier number of the Pseudo first-order time constant for the maximum temperature difference within the layer are presented in Fig. 19. The correlation reported by Kulacki and Emara [9] and Cheung's prediction [5] based on the boundary layer analysis are also shown in that figure. The present results give a much longer time than the time obtained from

Kulacki and Emara's correlation. This is partially due to the difference in the method of recording temperatures, which was discussed earlier.

Normalized step decreases in the Rayleigh number, $\frac{|\Delta Ra|}{\theta_{co_F}}$, versus the Fourier number of the pseudo first-order time constant for the minimum temperature difference within the layer are shown in Fig. 20 in conjunction with the correlation given by Kulacki and Emara [9]. Cheung's prediction [5] based on the boundary layer analysis for complete decay and transition from one state of steady convection to another, are also given in the same figure. The results of the present study give a much longer time than those of both Kulacki and Emara correlation, and Cheung's theoretical prediction. Cheung's prediction, however, indicates a longer time than the one obtained from correlation given by Kulacki and Emara. For the same step decrease in the normalized Rayleigh number, $\frac{\Delta Ra}{\theta_{co_F}}$, Cheung's prediction gives a slightly longer time for transition from one state of steady convection to another than for complete decay.

Measured and predicted temperature differences across the layer for a step increase and a step decrease in Rayleigh number versus the Fourier number are presented in Figs. 21 and 22, respectively. The present results, in both cases, are in fairly good agreement with these predictions, which are based on the boundary layer analysis. The final temperature differences observed experimentally, in both cases, are within three percent of Cheung's prediction. On the time scale, as mentioned previously, at the last stage of temperature development a 40% increase in the Fourier number introduces 0.1% change in temperature difference across the layer.

For the case of complete decay, the fractional change in temperature difference across the layer versus the normalized Fourier number is presented in Fig. 23 in conjunction with prediction of Cheung [5] and the experimental data reported by Kulacki and Nagle [14] and Kulacki and Emara [9]. It should be noted that the temperature development reported by Kulacki and Nagle was recorded by a glass encased thermocouple inserted into the center of the cell through a hole in the top plate, which is the same method reported by Kulacki and Emara. Initially, the results of Kulacki and Emara [9] and Cheung [5] indicate a much faster rate of temperature drop within the layer than the results reported by Kulacki and Nagle [14] and the present study. Thereafter, Kulacki and Emara, and Kulacki and Nagle indicate the completion of the decay at a time where the present study and Cheung's prediction indicates that temperature differences of 9% and 4% of initial values exist across the layer, respectively.

It should be noted that in Figs. 21, 22 and 23 for the early stages of temperature development, i.e. up to 15% to 20% of Fo_{max}, the measured temperature can be increased by approximately 15% due to delay in the thermocouple response for the developing flow measurements ($\Delta Ra > 0$).

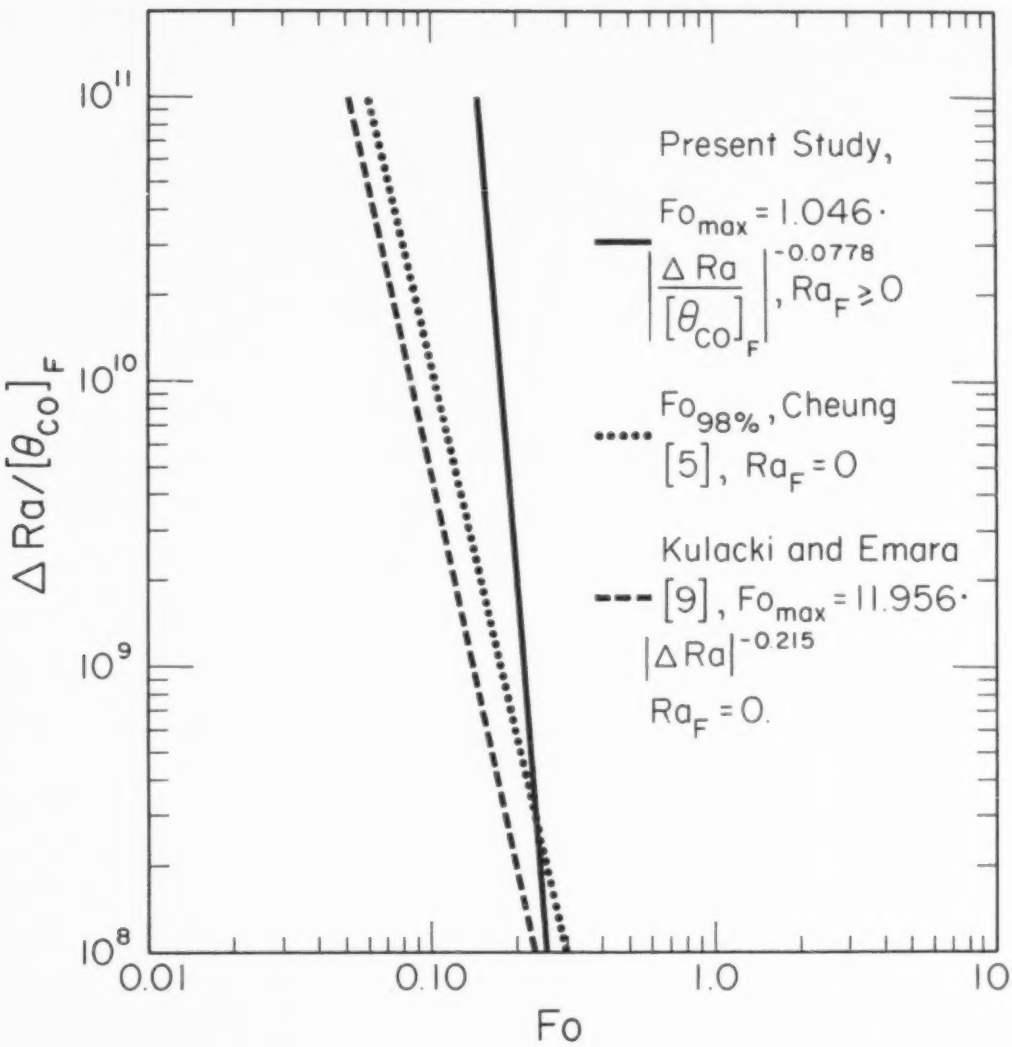

Figure 18. Correlations for Step Decrease in the Rayleigh Number versus the Fourier Number

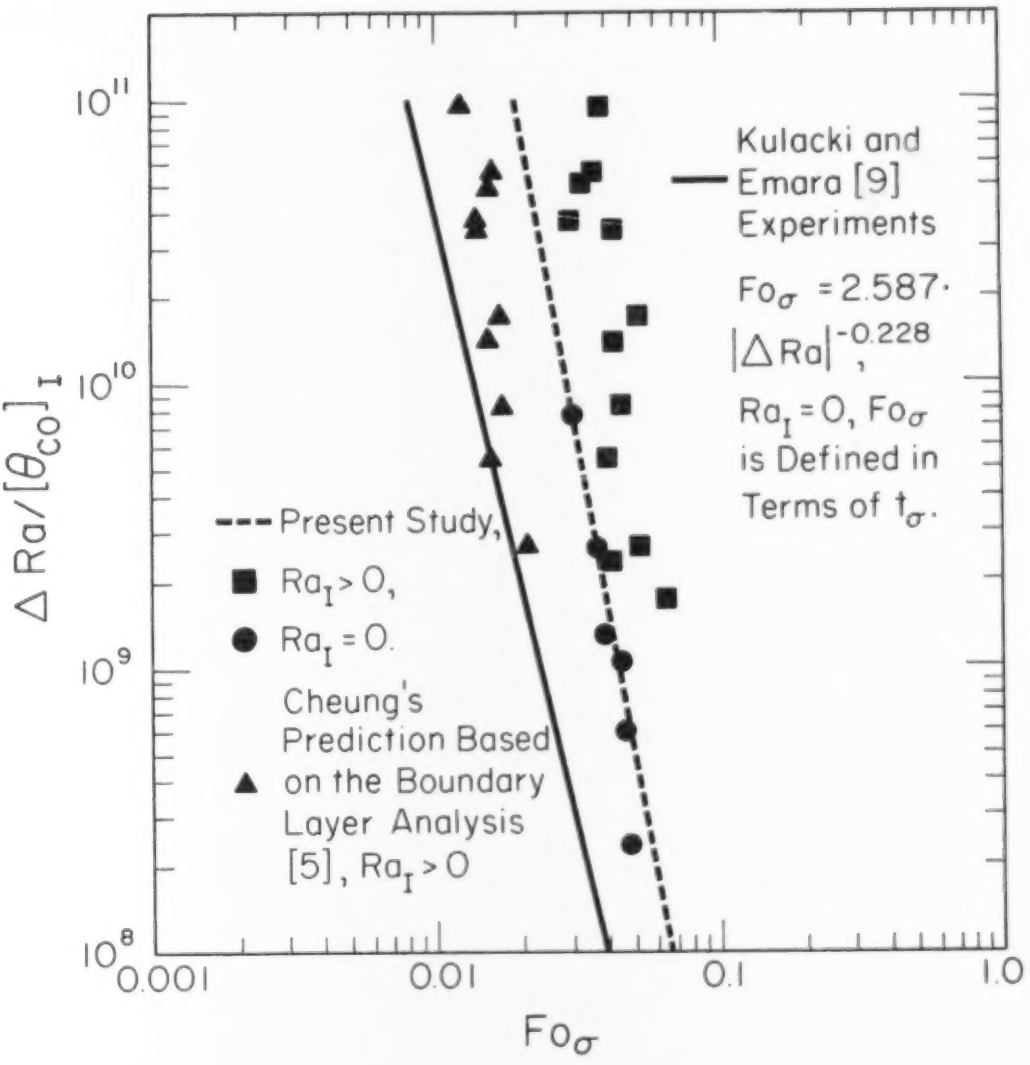

Figure 19. Normalized Step Increase in the Rayleigh Number versus the Fourier Number of the Pseudo First-Order Time Constant for the Maximum Temperature Difference Within the Layer

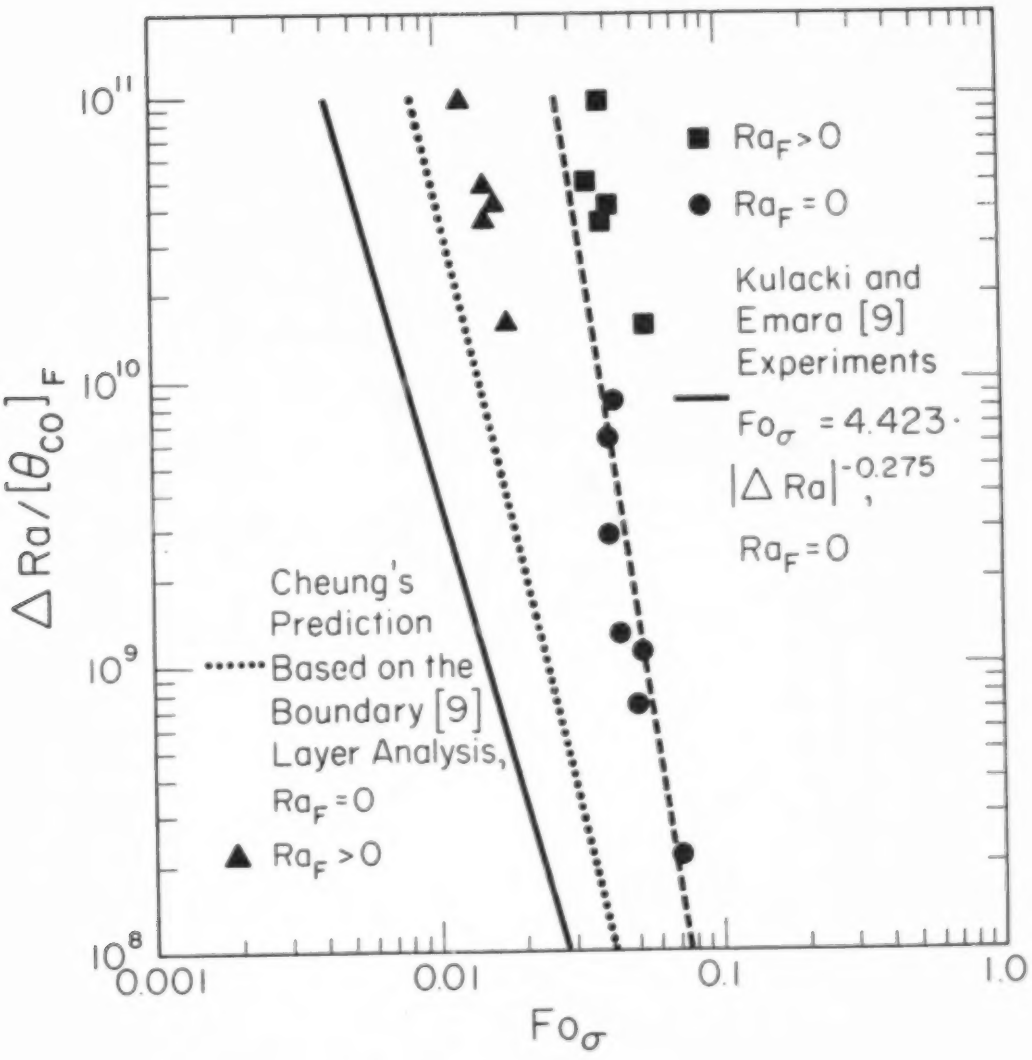

Figure 20. Normalized Step Decrease in the Rayleigh Number versus the Fourier Number of the Pseudo First-Order Time Constant for the Minimum Temperature Difference Within the Layer

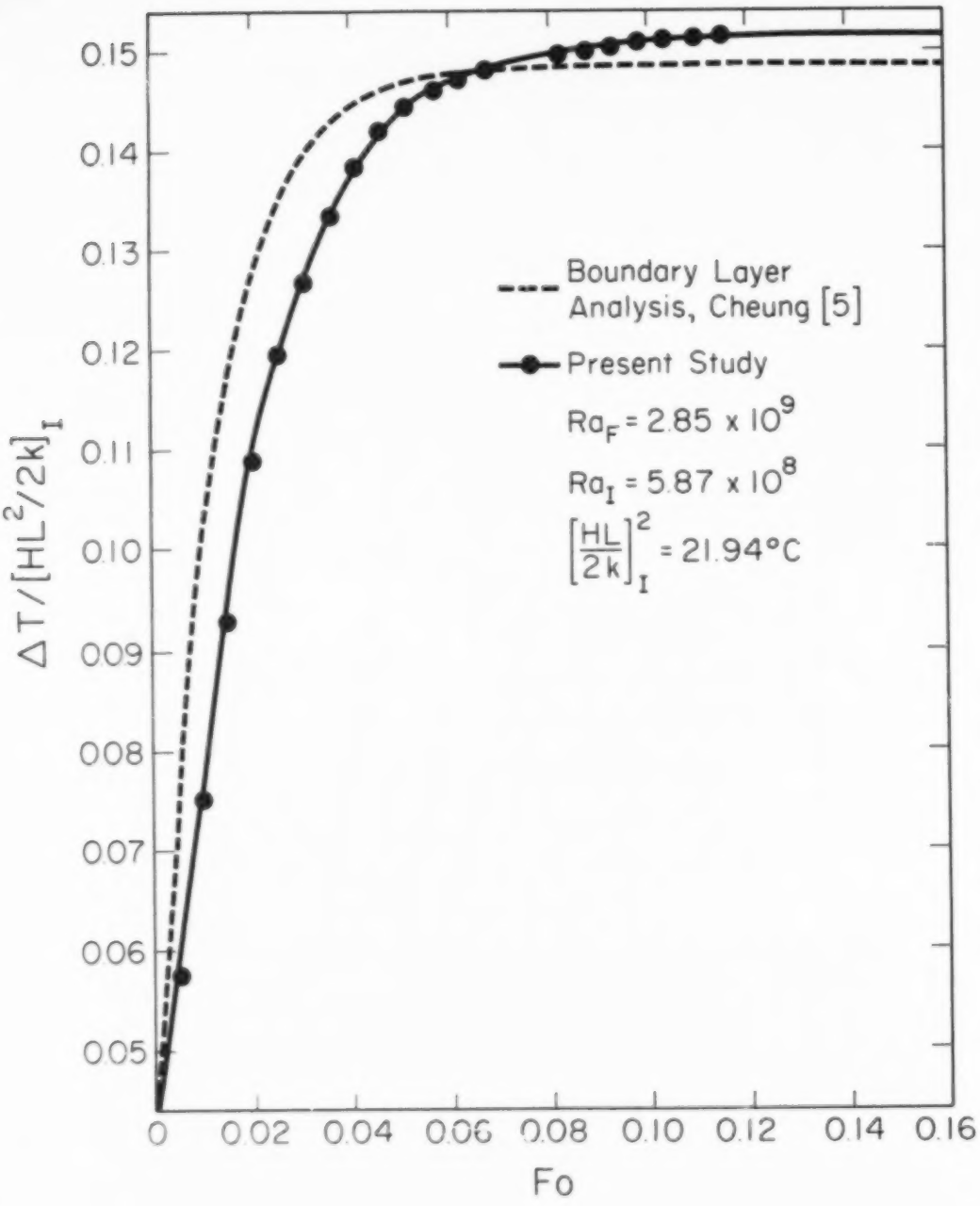

Figure 21. Measured and Predicted Temperature Difference Across the Layer for a Step Increase in Rayleigh Number. The Prediction is Based on the Boundary Layer Analysis of Cheung

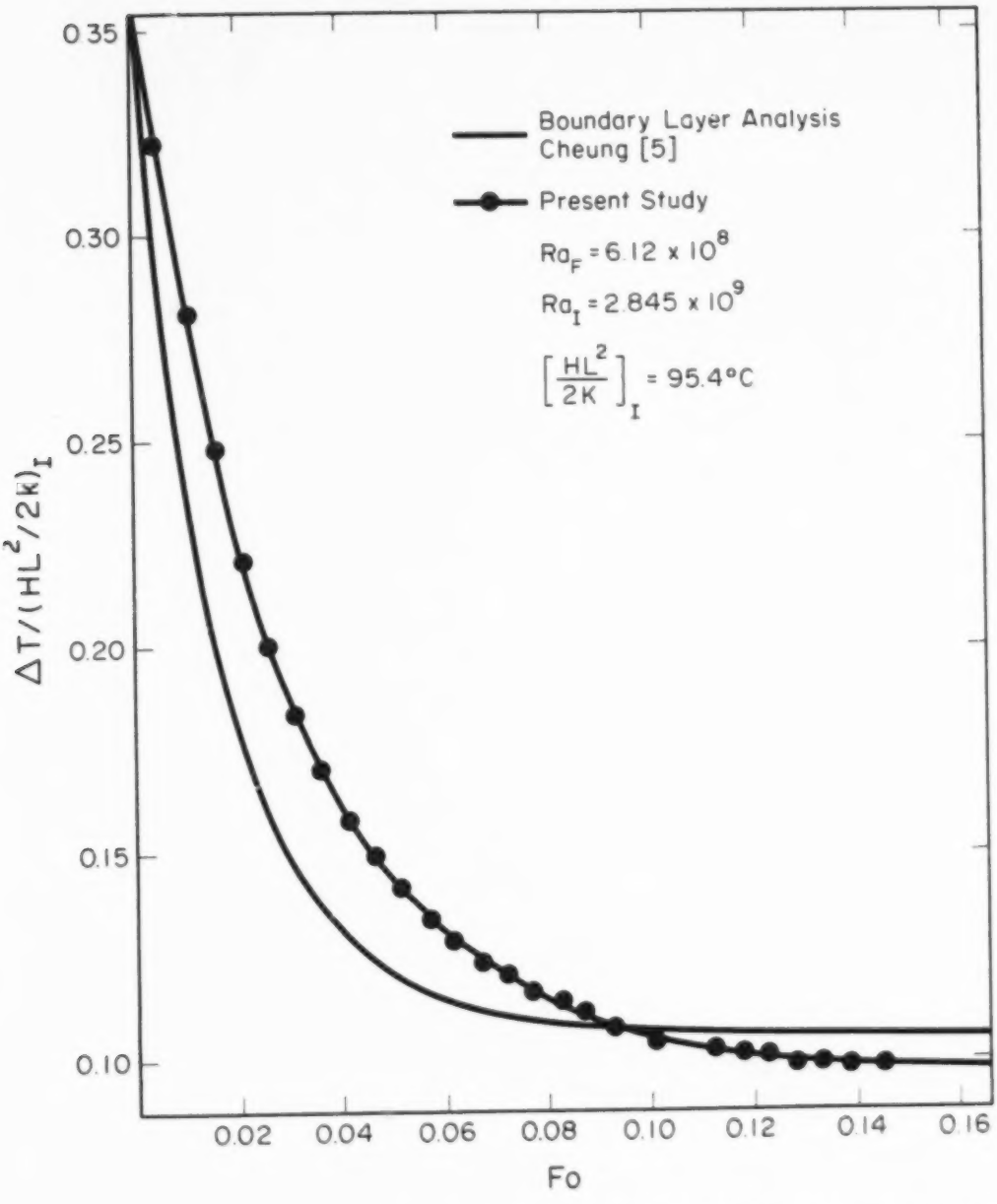

Figure 22. Measured and Predicted Temperature Difference Across the Layer for a Step Decrease in Rayleigh Number. The Prediction is Based on the Boundary Layer Analysis of Cheung

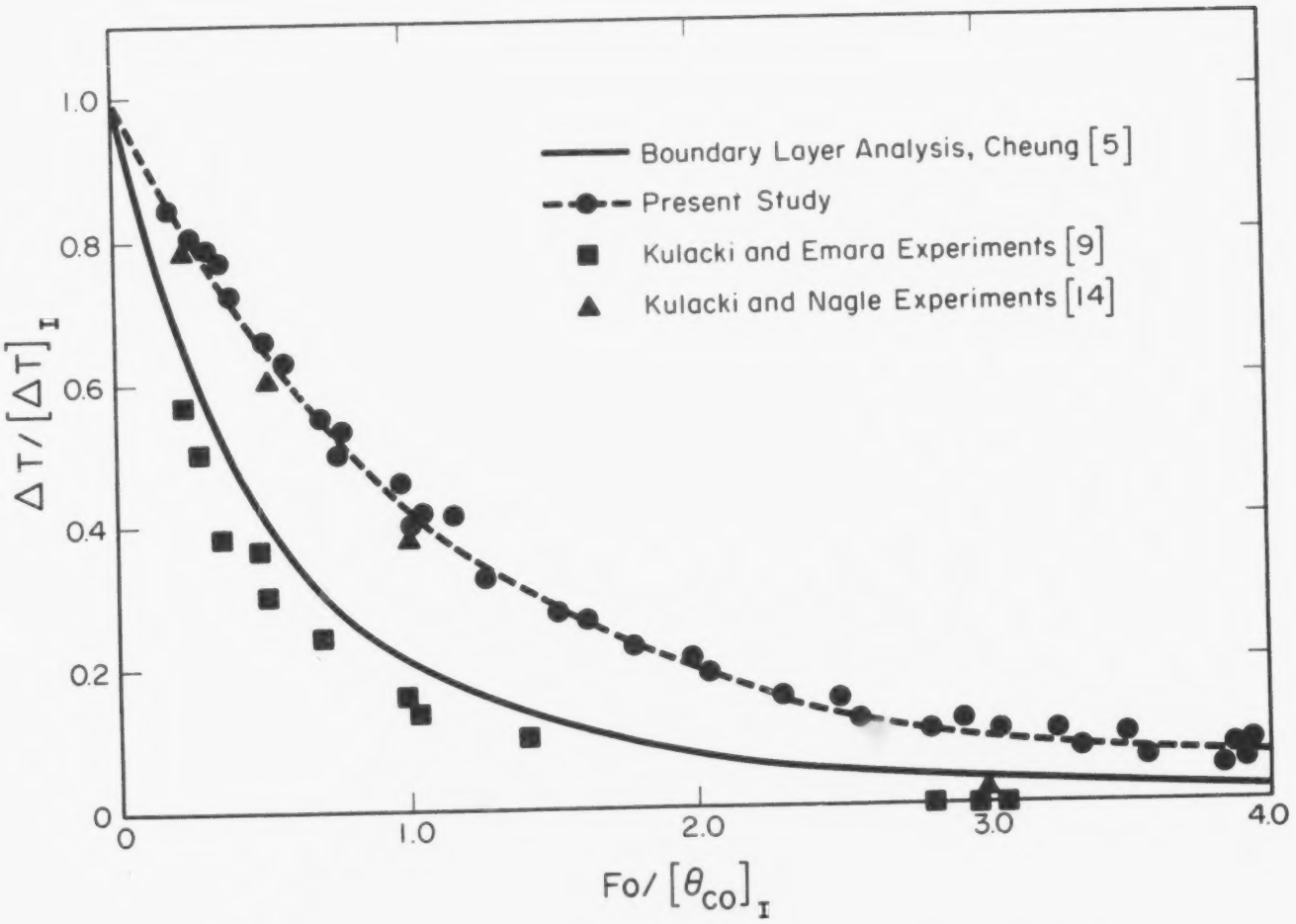

Figure 23. Complete Decay of the Turbulent Convection Flow

In decaying flow (Figs. 22 and 23), the measured temperature can be decreased by about 15% for the same reason at the same values of Fourier number. Appendix C contains analysis of errors which discusses time lags resulting from the effects of the thermal capacity of the lower boundary.

IV. CONCLUSION

An experimental study has been conducted on transient thermal convection wherein the transient processes in the fluid are initiated by a time-dependent volumetric energy source. In the present work, such a time dependency has been produced by changing the power input to the fluid such that the Rayleigh number is either greater or lower than its initial value. The major results of the study are steady-state heat transfer coefficients and time scales for developing and decaying convection. Data have been obtained for $3.65 \times 10^7 \leq Ra \leq 9.78 \times 10^9$ ($2.63 \times 10^4 \leq Ra/Ra_c \leq 7 \times 10^6$). Heat transfer coefficients are in very good agreement with those reported by Kulacki and Emara [9] (Figs. 5 and 6), while the measured time scales of the convection transients only partly substantiate the results of earlier work by Kulacki and Emara.

The measured flow development times in transient convection and the theoretical analysis of Cheung [5] indicate that a plot of the step change in the Rayleigh number $|\Delta Ra|$, versus the Fourier number, forms a family of curves with Ra_I, or θ_{co_I}, and Ra_F, or θ_{co_F}, as parameters for both developing and decaying flows (Figs. 8 to 15). When $Ra_I = 0$, the present results for developing flow essentially confirm the previous experimental results reported by Kulacki and Emara [9] (Fig. 14). The results obtained for the transition from one state of steady convection to another following a step increase in the Rayleigh number have been normalized and compared to the results of Kulacki and Emara [9] and Cheung [5]. The three results are in good agreement. This confirms the validity of the method of normalization (Fig. 16).

The data obtained for decaying flow, in normalized form, have been compared to the results reported by Kulacki and Emara [9] and the prediction of Cheung [5], which is based on a boundary layer analysis. The results of the present study and the results of Cheung indicate that a longer time is required for the completion of the transient compared to the time obtained from the correlation developed by Kulacki and Emara. A correlation between the Fourier number, and the normalized step decrease in Rayleigh number has been obtained in the following form.

$$Fo_{max,cooling} = 1.046 \left(\frac{\Delta Ra}{\theta co_F}\right)^{-0.0778}, \qquad (23)$$

where

$$10^8 \leq \frac{\Delta Ra}{\theta_{co_F}} \leq 10^{11} .$$

It is also concluded that for the same step change in Rayleigh number, a longer time is required for the completion of the transition in the case of decaying flow than that of the developing flow (Figs. 16 and 17). This phenomenon can physically be explained. In a fluid layer, with the same boundary conditions as in the present study, at steady-state convection, once a step increase in the volumetric energy source is applied the buoyancy force is uniformly increased. Therefore, the convective motion of the fluid particles is accelerated and the cooling rate at the top plate is increased with time. The bulk temperature of the fluid layer is increased until the excess energy generation in the fluid layer is absorbed and a new steady-state is reached. At this stage, if a step decrease of equal magnitude in the volumetric energy source is applied the buoyancy force is uniformly decreased. Therefore, the convective motion of the fluid particles is decelerated and the cooling rate at the top plate decreases with time. The energy which was stored in the fluid layer during the developing flow must be removed from the top surface until the bulk temperature of the fluid layer reaches its value at the initial steady-state.

In the developing flow process, the temperature difference across the fluid layer, and the step increase in the volumetric energy generation are the driving factors of the convective motion of the fluid particles. While, in the decaying process, in absence of a volumetric energy sink, the driving force behind the convective motion of the fluid particles is only the temperature difference across the fluid layer. These differences between the two processes indicate that one cannot be the exact inverse of the other, and therefore a difference between flow development and decay times is to be expected. Additional experimental and theoretical work would be needed, however, to sharpen the explanation of the different driving mechanisms for developing and decaying flow.

The present correlation for flow decay time, nevertheless, is in fair agreement with the results of Kulacki and Emara for very large time. For small time, experimental uncertainties (Appendix C) indicate a possible correction of 15% to 20% in temperature. This will bring the present results only slightly closer to the early flow development trends in temperature observed by Kulacki and Emara, where present data indicate a large first-order time constant. Thus, the present correlation for flow decay time may be considered an improvement of the earlier results reported by Kulacki and Emara.

It should be noted that it is more difficult to maintain the boundary condition at the lower surface (zero heat flux) in the case of decaying flow experiments than that of decaying flow. This is due to the fact that the energy stored in the bottom plate, while the layer is at steady-state, is released during the decaying flow experiments, thus effecting the temperature measurements. During the flow development however, the zero heat flux condition at the bottom plate is maintained by the energy generated through the heat guard. Both of these factors have been taken into consideration in the analysis of the effects of the thermal capacity of the lower boundary on the time lag in the measured

temperatures at the bottom of the fluid layer. The aforementioned estimates of a 15% to 20% correction on temperature and an 8% maximum correction in time scale of transient convection results from such a consideration.

APPENDIX A

THERMOPHYSICAL PROPERTIES OF THE FLUID

The thermophysical properties of the aqueous copper sulfate solution which served as the fluid medium in the convection cell were necessary for calculation of both the Rayleigh number and Nusselt number. However, sufficient data for the concentration dependence of such a solution does not exist and therefore property values were used as functions of temperature alone. Least squares polynomial fits as developed by Kulacki [5] were adapted for use in this thesis. This method of evaluating the thermophysical properties resulted in an error of approximately 1% in each property values.

The values used for the coefficient of volume expansion, β, were obtained by evaluating the quantity $(-1/\rho)(\partial\rho/\partial T)_p$, where the derivative was calculated as an integral part of the data reduction.

Table A-1 gives a summary of the thermophysical properties of water used in the present study.

Table A-1. Thermophysical Properties of Water

Temperature (^{o}C)	20	22	24	26	28	30	32	34	36	38	40
Property											
ρ	.998	.998	.997	.997	.996	.996	.995	.994	.994	.993	.992
$\nu \times 10^2$	1.01	.963	.919	.878	.840	.804	.771	.740	.711	.684	.659
$\beta \times 10^3$	.206	.226	.249	.266	.284	.301	.318	.334	.349	.364	.377
C_p	.999	.999	.998	.998	.998	.998	.998	.998	.998	.998	.998
$k \times 10^2$	.1431	.1437	.1444	.1451	.1458	.1464	.1471	.1478	.1484	.1491	.1497

Note that units are: Density, gm/cm^3

Viscosity, cm^2/sec

Beta, ^{o}C-1

Specific Heat, cal/gm ^{o}C

Thermal Conductivity, cal/cm-sec ^{o}C

APPENDIX B

EXPERIMENTAL DATA

Table B-1. Steady State Heat Transfer Data, W = 0.4%.

Run	L (cm)	P (W)	ΔT (°C)	θ_{co_F}	Pr	Ra	Nu_1
1	10.16	2.025	0.196	0.074	6.37	5.17×10^7	26.94
2	10.16	2.107	0.231	0.0846	5.87	6.41	23.58
3	10.16	2.8	0.297	0.0814	6.24	7.42	24.495
42	7.62	3.52	0.259	0.076	5.62	3.69	25.114
43	7.62	3.52	0.289	0.0848	5.66	3.65	22.62
4	10.16	4.025	0.372	0.071	6.34	1.04×10^8	28.237
5	10.16	4.148	0.308	0.057	5.85	1.27	34.74
6	10.16	5.6	0.432	0.060	6.25	1.47	33.316
7	10.16	8.448	0.511	0.0468	5.82	2.67	42.566
8	10.16	11.2	0.722	0.0495	6.17	3.06	40.20
9	10.16	16.616	0.877	0.0409	5.76	5.26	48.6
10	10.16	24.96	1.442	0.0445	6.00	7.24	44.705
22	10.16	17.89	0.976	0.042	5.74	5.72	47.33
23	10.16	9.024	0.5822	0.05	5.81	2.81	39.818
38	10.16	17.1	0.9615	0.0437	5.53	5.87	45.397
30	10.16	8.35	0.558	0.0514	6.11	2.34	38.837
40	10.16	17.775	1.058	0.0463	5.52	6.12	42.886
44	7.62	23.1	1.346	0.0652	5.58	1.86	30.44
11	10.16	33.271	1.644	0.0383	5.62	1.10×10^9	51.76
12	10.16	47.83	2.6	0.042	5.79	1.49	47.256
13	10.16	67.869	3.172	0.0364	5.39	2.44	54.68
14	10.16	104.154	5.3	0.0395	5.36	3.8	50.415

Table B-1 (continued)

Run	L (cm)	P (W)	ΔT (°C)	θ_{co_F}	Pr	Ra	Nu_1
15	10.16	143.4	5.899	0.0323	4.97	5.97	61.655
17	10.16	199.0	7.625	0.030	4.74	8.98	65.87
18	10.16	212.75	7.9515	0.030	4.7	9.78	66.645
19	10.16	157.2	6.33	0.0317	4.91	6.69	62.91
20	10.16	75.9	3.432	0.034	5.34	2.87	58.536
21	10.16	36.45	1.855	0.039	5.59	1.23	50.50
24	10.16	36.4	1.875	0.04	5.42	1.30	49.64
26	10.16	35.2	1.779	0.039	5.92	1.05	51.142
27	10.16	77.14	3.232	0.0325	5.7	2.49	61.446
28	10.16	36.4	1.808	0.0384	5.91	1.09	52.05
32	10.16	80.7	3.5	0.0337	5.66	2.64	59.323
34	10.16	155.168	6.16	0.031	5.09	6.21	63.93
36	10.16	176.0	6.817	0.0306	4.77	7.87	65.241
39	10.16	74.594	3.317	0.0348	5.22	2.85	57.273

Table B-2. Data for Developing Flow for a Step Increase in Ra. $R_a = 0$, $\theta_{c\sigma_I} = 1$.

Run	ΔRa	θ_{co_F}	t_{max} (hr)	t_σ (hr)	Fo_{max}	Fo_σ
1	5.17×10^7	0.074	----	1.2	-----	0.061
2	6.41	0.0846	----	0.9	-----	0.051
3	7.42	0.0814	----	1.1	-----	0.056
24	1.30×10^9	0.040	1.8	0.75	0.093	0.039
26	1.05	0.039	2.6	0.88	0.132	0.045
30	2.34×10^8	0.0514	2.8	0.95	0.142	0.048
32	2.64×10^9	0.0337	----	0.72	-----	0.037
36	7.87	0.0306	1.5	0.6	0.078	0.031
38	5.87×10^8	0.0437	2.8	0.9	0.144	0.046
43	3.65×10^7	0.0848	3.0	0.9	0.273	0.082

Table B-3. Data for Decaying Flow for a Step Decrease in Ra. $Ra_F = 0$, $\theta_{co_F} = 1$.

Run	ΔRa	θ_{co_I}	t_{max} (hr)	t_σ (hr)	Fo_{max}	Fo_σ
25	1.29×10^9	0.04	3.6	0.87	0.184	0.044
29	1.1	0.0384	4.4	1.05	0.223	0.053
31	2.34×10^8	0.0514	5.2	1.4	0.263	0.0708
33	2.75×10^9	0.0336	3.8	0.8	0.193	0.0406
35	6.17	0.0311	4.0	0.8	0.203	0.0406
37	8.4	0.029	3.6	0.83	0.184	0.042
41	6.12×10^8	0.0463	3.6	1.0	0.1836	0.051

Table B-4. Data for Developing Flow for a Step Increase in Ra., $Ra_I > o$.

Run	Ra_I	Ra_F	ΔRa	$[\frac{HL^2}{2k}]_I$	θ_{co_I}	$[\frac{HL^2}{2k}]_F$	θ_{co_F}	$\frac{\Delta Ra}{\theta_{co_I}}$	t_{max} (hr)	t_σ (hr)	Fo_{max}	Fo_σ
7	$1.27x10^8$	$2.67x10^8$	$1.40x10^8$	5.364	0.0574	10.92	0.0468	$2.44x10^9$	----	0.8	------	0.041
8	1.47	3.06	1.59	7.22	0.060	14.568	0.0495	2.65	2.3	1.05	0.117	0.053
9	2.67	5.26	2.59	10.92	0.0468	21.445	0.0409	5.53	1.72	0.8	0.088	0.041
10	3.06	7.24	4.18	14.568	0.0496	32.367	0.0445	8.43	1.9	0.9	0.097	0.046
11	5.26	$1.10x10^9$	5.74	21.445	0.0409	42.851	0.0383	$1.40x10^{10}$	2.0	0.85	0.103	0.044
12	7.24	1.49	7.66	32.368	0.0445	61.797	0.042	1.72	2.4	1.05	0.122	0.053
13	$1.10x10^9$	2.44	$1.34x10^9$	42.852	0.0384	87.076	0.0364	3.49	1.4	0.85	0.072	0.043
14	1.49	3.8	2.31	61.797	0.0421	134.10	0.0395	5.49	1.6	0.7	0.083	0.0361
15	2.44	5.97	3.53	87.076	0.0364	182.387	0.0323	9.7	1.6	0.75	0.083	0.039
27	1.05	2.49	1.44	45.58	0.039	99.504	0.0325	3.7	1.4	0.6	0.072	0.031
39	$5.87x10^8$	2.85	2.26	21.988	0.0437	95.35	0.0348	5.17	1.5	0.65	0.0775	0.0335
44	$3.70x10^7$	$1.86x10^8$	$1.49x10^8$	3.403	0.0848	20.64	0.0652	$1.76x10^9$	1.5	0.62	0.159	0.066

Table B-5. Data for Decaying Flow for a Step Decrease in Ra., $Ra_F > 0$.

Run	Ra_I	Ra_F	ΔRa	$[\frac{HL^2}{2k}]_I$	θ_{co_I}	$[\frac{HL^2}{2k}]_F$	θ_{co_F}	$\frac{\Delta Ra}{\theta_{co_F}}$	t_{max} (hr)	t_σ (hr)	Fo_{max}	Fo_σ
19	9.77×10^9	6.68×10^9	3.09×10^9	2.69	0.0295	199.7	0.0317	9.75×10^{10}	3.2	0.86	0.146	0.039
20	6.68	2.87	3.81	199.7	0.0317	100.8	0.034	1.12×10^{11}	3.0	0.9	0.155	0.0465
21	2.87	1.23	1.64	100.8	0.034	47.1	0.039	4.2×10^{10}	3.0	0.8	0.154	0.0411
22	1.23	5.72×10^8	1.68×10^8	47.1	0.039	23.2	0.042	1.57	3.2	1.1	0.164	0.0563
28	2.53	1.1×10^9	1.43×10^9	99.5	0.032	47.1	0.0384	3.72	3.0	0.8	0.153	0.0408
40	2.84	6.12×10^8	2.23	95.4	0.0348	22.8	0.0463	4.81	2.8	0.69	0.144	0.0355

APPENDIX C

ANALYSIS OF EXPERIMENTAL ERRORS

The Rayleigh number and Nusselt number are subject to accidental and systematic errors because of uncertainties in the parameters used to calculate these dimensionless quantities.

Accidental error was eliminated by taking repeated measurements and taking the arithmetic mean value for those readings. Assuming that this method is sufficient to eliminate the accidental error, it was assumed that all error resulted from systematic error.

Systematic errors include uncertainties in the thermophysical properties of the electrolyte solution, convection cell geometrical dimensions, temperature measurement readings of the voltmeter and ammeter and the power lost through the bottom plate and side walls. Each form of error will be considered in turn. It is assumed that the convection cell is perfectly aligned with the horizon.

Applying the law of summation of fractional errors [20], the fractional error for the Rayleigh number is,

$$f_{Ra} = f_{properties} + f_{geometric} + f_{power},$$

and the fractional error in the Nusselt number is,

$$f_{Nu} = f_{properties} + f_{geometric} + f_{power} + f_{temperature}.$$

The estimated uncertainties in the thermophysical property values are given by Appendix A.

The Mylar covering of the aluminum top plate had an uncertainty of 0.00127 cm, which when added to the 0.00127 cm uncertainty of the Plexiglas spacers, resulted in an uncertainty of 0.0025 cm in L. The horizontal dimension of the convection cell is known to within 0.0127 cm. An error of 0.5% was used for all other geometrical measurements.

The combined uncertainties in the thermophysical properties and geometrical factors produced an uncertainty of 4% to 6% in the experimental Rayleigh number and 1% to 3% in the experimental Nusselt number.

The errors of both the digital multimeter and the ammeter were rated at 0.5% of the reading. Allowing for error of reading, the outputs of these instruments, the estimated uncertainty in power consumption was 2% for the range of Rayleigh number in this study.

The calculated value of energy transport through the bottom plate and side walls was less than 1% of the measured power input for each run.

It is not possible to systematically determine the amount of error in this calculated energy loss because nominal property values supplied by the manufacturer were used in the calculation. Thus, the actual value of energy transported through the top plate was taken to be within 1% of the calculated value.

The uncertainties in the thermocouple output, potentiometer reading and conversion from emf to degrees Celsius resulted in the error of the measured temperature to be 1%. This gives the most probable error in the temperature difference at 1.5%.

Summing all fractional errors, the error in the Rayleigh number is 6% to 8% and the error in the Nusselt number is 3.5% to 5.5%.

In the measurement of the temperature development, the uncertainty in reading the output of the strip chart recorder is $\pm$ 0.5% for both temperature and elapsed time. The temperature development at the bottom of the fluid layer is recorded by a thermocouple placed in the bottom plate 0.128 cm from its surface, assuming that it represents the temperature development at the interface of the fluid layer and the bottom plate with a delay in response. In order to estimate the error induced on the transient temperature measurement by this delay in the response of the thermocouple, an analysis was made of transient heat conduction in the lower boundary of the convection cell. Initially, the lower plate is at uniform temperature (i.e., $T(z,o) = T_i$). At time greater than zero, the top surface is held at a temperature as a function of time, i.e., $T(1,t) = T_i \pm T_i \cdot t$, where the thickness of the plate is taken as unity. The surface at the bottom of the plate is assumed adiabatic. This problem is analytically investigated for the temperature development at 0.128 cm from the top surface of the plate, which is the position of the thermocouple. For short times, i.e., up to 15% to 20% of Fo_{max}, where the assumed linear dependence of surface temperature on time is approximately valid, it is estimated that the actual temperature input is about 15% larger than the measured temperature in the case of developing flow. For decaying flow, the temperature lags the true value by about 15%. In terms of real time, the delay in response is about twelve minutes which is approximately 4% to 8% of the maximum times measured. The maximum Fourier numbers are estimated to be accurate within 6% to 10%. While this level of experimental uncertainty is higher than for measured Nusselt and Rayleigh numbers, it is not considered unreasonable in view of the experimental method used.

BIBLIOGRAPHY

1. Anderson, E. E., "Radiative Heat Transfer in Molten UO_2 Based on the Rosseland Diffusion Method," Nuclear Technology, Vol. 30, pp. 65-70 (1976).

2. Chandrashekhar, S., Hydrodynamic and Hydromagnetic Stability, Oxford, London, 1961.

3. Cheung, F. Bl, "Correlation Equations for Turbulent Convection in a Horizontal Fluid Layer Heated Internally and Below," ASME Journal of Heat Transfer, Vol. 100, pp. 16-22 (1978).

4. Cheung, F. Bl, "The Boundary Layer Behavior in Transient Turbulent Thermal Convection Flow," Personal Communication with F. A. Kulacki, June 1979.

5. Cheung, F. B., "Turbulent Natural Convection in a Horizontal Fluid Layer with Time Dependent Volumetric Energy Sources," Paper No. 78-HT-6, AIAA-ASME Thermophysics and Heat Transfer Conference, Palo Alto, Ca., 1978.

6. Emara, A. A., On Thermal Convection With Internal Heating In Fluid Layers, Ph.D. Dissertation, The Ohio State University, 1977.

7. Krishnamurty, R., "Finite Amplitude Convection with Changing Mean Temperature. Part 2., An Experimental Test of the Theory," Journal of Fluid Mechanics, Vol. 33, pp. 457-463 (1968).

8. Kulacki, F. A., Emara, A. A., Korpela, S. A., Lambha, N. K. and Min, J. H., "Natural Convection with Internal Energy Sources: Some Recent Experimental and Numerical Results with Post-Accident Heat Removal Applications," Proceedings of the Third Post-Accident Heat Removal Information Exchange," Argonne National Laboratory Report ANL-78-10, L. Baker, Jr. and J. Bingle, Eds., pp. 101-113 (1978).

9. Kulacki, F. A. and Emara, A. A., "Steady and Transient Thermal Convection in a Fluid Layer with Uniform Volumetric Energy Sources," Journal of Fluid Mechanics, Vol. 83, pp. 375-395 (1977).

10. Kulacki, F. A. and Goldstein, R. J., "Eddy Heat Transport in Thermal Convection with Volumetric Energy Sources," Proceedings of the Fifth International Heat Transfer Conference, Vol. 3, pp. 64-68, Tokyo, 1974.

11. Kulacki, F. A. and Goldstein, R. J., "Hydrodynamic Instability in Fluid Layers with Uniform Volumetric Energy Sources," Applied Scientific Research, Vol. 31, pp. 81-109 (1975).

12. Kulacki, F. A. and Goldstein, R. J. "Thermal Convection in a Horizontal Fluid Layer with Uniform Volumetric Energy Sources," Journal of Fluid Mechanics, Vol. 55, No. 2, pp. 271-278 (1972).

13. Kulacki, F. A., Min, J. H., Hguyen, A. T. and Keyhani, M., "Steady and Transient Natural Convection in Single and Multi-Fluid Layers with Heat Generation," Proceedings of Post-Accident Heat Removal Information Exchange, Ispra, Italy, 1978.

14. Kulacki, F. A. and Nagle, M. E., "Natural Convection in a Horizontal Fluid Layer with Volumetric Energy Sources," ASME Journal of Heat Transfer, Vol. 97, pp. 204-211 (1975).

15. Kulacki, F. A., Thermal Convection in a Horizontal Fluid Layer with Uniform Volumetric Energy Sources, Ph.D. Dissertation, University of Minnesota, 1971.

16. Lord Rayleigh, "On Convection Currents in a Horizontal Layer of Fluid When the Higher Temperature is on the Under Side," Philosophical Magazine, Vol. 32, pp. 529-546 (1916).

17. McKenzie, D. P., Roberts, J. M., and Weiss, N. O., "Convection in the Earth's Mantle; Towards a Numerical Simulation," Journal of Fluid Mechanics, Vol. 62, pp. 465-538 (1974).

18. Min, J. H. and Kulacki, F. A., "An Experimental Study of Thermal Convection with Volumetric Energy Sources in a Fluid Layer Bounded From Below by a Segment of a Sphere," Proceedings of the Sixth International Heat Transfer Conference, Vol. 5, pp. 155-160, National Research Council of Canada, 1978.

19. Schwiderski, E. W. and Schwab, J. A., "Convection Experiments with Electrolytically Heated Fluid Layers," Journal of Fluid Mechanics, Vol. 48, pp. 703-720 (1971).

20. Topping, J., Errors of Observation and Their Treatment, Third Ed., Chapman and Hall, London, 1955.

21. Tritton, D. J., "Internally Heated Convection in the Atmosphere of Venus and in the Laboratory," Nature, London, Vol. 257, pp. 110-111 (1975).

22. Tritton, D. J. and Zaraga, M. N., "Convection in Horizontal Layers with Heat Generation Experiments," Journal of Fluid Mechanics, Vol. 30, pp. 1-21 (1907).

23. Turcotte, D. L. and Oxburgh, E. R., "Mantle Convection and the New Global Tectonic," Annual Reviews of Fluid Mechanics, Vol. 4, pp. 33-68 (1972).

NRC FORM 335 (7-77) U.S. NUCLEAR REGULATORY COMMISSION

BIBLIOGRAPHIC DATA SHEET

1. REPORT NUMBER (Assigned by DDC): NUREG/CR-1173

4. TITLE AND SUBTITLE (Add Volume No., if appropriate)

An Experimental Study of Turbulent Thermal Convection With Time-Dependent Volumetric Energy Sources

2. (Leave blank)

3. RECIPIENT'S ACCESSION NO.

7. AUTHOR(S)

Majid Keyhani and Francis A. Kulacki

5. DATE REPORT COMPLETED: MONTH October YEAR 1979

9. PERFORMING ORGANIZATION NAME AND MAILING ADDRESS (Include Zip Code)

The Ohio State University Research Foundation
1314 Kinnear Road
Columbus, Ohio 43212

DATE REPORT ISSUED: MONTH YEAR

6. (Leave blank)

8. (Leave blank)

12. SPONSORING ORGANIZATION NAME AND MAILING ADDRESS (Include Zip Code)

U.S. Nuclear Regulatory Commission
Washington, D.C. 20555

10. PROJECT/TASK/WORK UNIT NO

11. CONTRACT NO.

NRC-04-74-149

13. TYPE OF REPORT: Topical

PERIOD COVERED (Inclusive dates): September 1978 to August 1979

15. SUPPLEMENTARY NOTES

14. (Leave blank)

16. ABSTRACT (200 words or less)

Transient natural convection in a horizontal layer of dilute aqueous electrolyte with internal heat generation is experimentally investigated. The layer is bounded from below by a rigid, zero heat flux surface and from above by a rigid, isothermal surface. The nature of the developing and decaying convection processes in the layer is observed. Initially, the layer is at steady-state with power input, or Rayleigh number, greater or equal to zero. The time needed for the layer to reach its final steady-state following a step change in power input is obtained. For a step decrease in Rayleigh number, the resulting decaying process is found to require more time than the developing process resulting from a step increase in Rayleigh number of equal magnitude. Comparisons are made with existing experimental data for the case of a power "on-off" step function and with an analysis based on a boundary layer approximation for the case of developing and decaying processes with initial Rayleigh number greater than zero.

17. KEY WORDS AND DOCUMENT ANALYSIS

17a. DESCRIPTORS

Natural Convection Heat Transfer

17b. IDENTIFIERS/OPEN-ENDED TERMS

Post-accident heat removal

18. AVAILABILITY STATEMENT: Unlimited

19. SECURITY CLASS (This report): Unclassified

21. NO. OF PAGES

20. SECURITY CLASS (This page)

22. PRICE $

NRC FORM 335 (7-77)

UNITED STATES
NUCLEAR REGULATORY COMMISSION
WASHINGTON, D. C. 20555

OFFICIAL BUSINESS
PENALTY FOR PRIVATE USE, $300

POSTAGE AND FEES PAID
U.S. NUCLEAR REGULATORY
COMMISSION